frontiers | Frontiers in Immunology

TYPE Original Research
PUBLISHED 20 December 2024
DOI 10.3389/fimmu.2024.1493840

OPEN ACCESS

EDITED BY
Jorge Galindo-Villegas,
Nord University, Norway

REVIEWED BY
Rocio Leiva Rebollo,
Icahn School of Medicine at Mount Sinai, United States
Ingvill Jensen,
UiT The Arctic University of Norway, Norway

*CORRESPONDENCE
Tomáš Korytář
tkorytar@paru.cas.cz

RECEIVED 09 September 2024
ACCEPTED 20 November 2024
PUBLISHED 20 December 2024

CITATION
Chan JTH, Picard-Sánchez A, Dedić N, Majstorović J, Rebl A, Holzer AS and Korytář T (2024) Immunological memory in a teleost fish: common carp IgM$^+$ B cells differentiate into memory and plasma cells.
Front. Immunol. 15:1493840.
doi: 10.3389/fimmu.2024.1493840

Immunological memory in a teleost fish: common carp IgM$^+$ B cells differentiate into memory and plasma cells

Justin Tze Ho Chan[1,2], Amparo Picard-Sánchez[1], Neira Dedić[1,3,4], Jovana Majstorović[1,5], Alexander Rebl[6], Astrid Sibylle Holzer[1,2] and Tomáš Korytář[1,4,7]*

[1]Laboratory of Fish Protistology, Institute of Parasitology, Biology Centre, Czech Academy of Sciences, České Budějovice, Czechia, [2]Fish Health Division, University of Veterinary Medicine, Vienna, Austria, [3]Department of Botany and Zoology, Faculty of Science, Masaryk University, Brno, Czechia, [4]Laboratory of Fish Immunology, Institute of Parasitology, Biology Centre, Czech Academy of Sciences, České Budějovice, Czechia, [5]Faculty of Science, University of South Bohemia, České Budějovice, Czechia, [6]Working Group Fish Genetics, Research Institute for Farm Animal Biology, Dummerstorf, Germany, [7]South Bohemian Research Centre of Aquaculture and Biodiversity of Hydrocenoses, Institute of Aquaculture and Protection of Waters, Faculty of Fisheries and Protection of Waters, University of South Bohemia, České Budějovice, Czechia

From ancient cold-blooded fishes to mammals, all vertebrates are protected by adaptive immunity, and retain immunological memory. Although immunologists can demonstrate these phenomena in all fish, the responding cells remain elusive, without the tools to study them nor markers to define them. Fundamentally, we posited that it is longevity that defines a memory cell, like how it is antibody production that defines a plasma cell. We infected the common carp with *Sphaerospora molnari*, a cnidarian parasite which causes seasonal outbreaks to which no vaccine is available. B cells proliferated and expressed gene signatures of differentiation. Despite a half-year gap between EdU labeling and sampling, IgM$^+$ B cells retained the thymidine analogue, suggesting that these are at least six-month-old resting memory cells stemming from proliferating precursors. Additionally, we identified a lymphoid organ-resident population of plasma cells by the exceptional levels of IgM they express. Thus, we demonstrate that a teleost fish produces the lymphocytes key to vaccination success and long-term disease protection, supporting the idea that immunological memory is observable and universal across vertebrates.

KEYWORDS

humoral memory, antibody, immunoglobulin, myxozoa, antibody-secreting cell (ASC)

1 Introduction

Over 500 million years ago, ancient cold-blooded fishes emerged along with adaptive immunity (1). Together with immunological memory (2), they form the basis of natural immunity, and vaccinology. These phenomena manifest as secretion of microbe-specific agglutinins, memory responses to antigen, accelerated rejection of allografts, and acquired protection from reinfection. They are observable and common to all fish including jawless fish (3, 4), cartilaginous fish (5–7), and bony fish (8, 9), with published reports dating back to over 80 years ago (10). Nowadays, we routinely observe adaptive immune and memory responses in a variety of fish species (11–15). Studying how these responses manifest promises solutions for preventing disease in fish. However, despite fish immunology coming to maturity, driven by comparative immunology and the importance of certain species to aquaculture, we still face difficulties identifying and studying the cells and mechanisms responsible for these phenomena.

It is especially difficult to identify homologous and functional molecules, cells and mechanisms in teleost fishes due to their rich diversity, evolutionary history and distance. For example, although the single-cell RNA sequencing of grass carp B cells identified plasma cells (16), there was a glaring absence of any population that corresponds to memory B cells. Fundamentally, it is phenomena such as longevity and antibody secretion (11–15, 17, 18) that are observed time and time again rather than any specific phenotypic marker or mechanism. Therefore, it is from this angle that we studied the common carp B cell response, and searched for memory B and plasma cell analogues.

We leveraged our laboratory model of *Cyprinus carpio* with the myxozoan (Cnidaria) parasite *Sphaerospora molnari* (19, 20). The myxozoans are ancient cnidarians that have co-evolved with and cycle between invertebrate and fish hosts. They cause economically important seasonal outbreaks in both wild and farmed fish stocks. In addition to the historical uncertainty over their phylogeny (21–23), the Myxozoa are also a scientific metazoan oddity due to adaptations such as one species losing the capacity for mitochondrial respiration (24). Generally, B cells respond strongly to myxozoan infections with proliferation and antibody production (25, 26). Myxozoan infections potentially elicit polyreactive antibodies (25); they induce distinct transcriptional signatures that frequently include *il10* upregulation (26–28); infections are ultimately chronic and latent (29). These features of both the host response and the pathogenesis of myxozoan infections led us to question whether the B cell response elicits antibodies that mitigate disease and produces differentiated memory B and plasma cells that provide long-term protection. In other words, we investigated whether the B cell response is protective and productive.

In the present study, by removing B cells via immunosuppression (19, 30–32), we provide evidence that B cells and antibodies limit the otherwise severe parasitemia and disease. Although we measured proliferation via incorporation of the thymidine analogue (5-ethynyl-2′-deoxyuridine, EdU) and detected gene signatures that indicate a productive B cell response, there are currently no specific phenotypic markers nor reagents to directly detect memory B cells. Thus, we relied on a single anti-carp IgM monoclonal antibody at our disposal. As described by Shibasaki et al. in a recent report of a germinal center analogue in fish, EdU labels cells engaged in an immune response and germinal center activity (33). It is through tracing the long-term retention of the thymidine analogue EdU that we directly detected resting memory B cells. A corticosteroid-resistant, enlarged, and head/anterior kidney lymphoid organ-resident B cell population expressing high levels of cytosolic IgM may represent plasma cells that constitutively secrete antibodies after resolution of the acute immune response. In this complex teleost host-myxozoan parasite interaction, humoral memory of a past infection, and protection are achievable. As our methodology is based on fundamental phenotypes of memory B and plasma cells rather than any homologous markers, it is applicable towards the study of these subpopulations and these phenomena in other species.

2 Results

2.1 The B cell compartment expands and produces *S. molnari*-specific antibodies that limit parasitemia

To study the role played by B cells and the antibody response in *S. molnari* infection, we compared B cell-sufficient and B cell-depleted common carp throughout infection with the parasite. We previously revealed the most severe form of *S. molnari* infection via immunosuppression with the synthetic corticosteroid triamcinolone acetonide (19, 30–32). Here, we demonstrate that immunosuppression completely depletes the peripheral IgM^+ B cell population within 3 days of administration (Figure 1) and allows us to study the outcome of infection in the absence of B lymphocytes.

Fish were either not treated with the corticosteroid (immunosufficient) or immunosuppressed with it (IS). Under each of these two conditions, we further subdivided fish into three groups receiving one of three ten-fold diluted doses of diethylaminoethyl (DEAE) cellulose-purified *S. molnari* blood-stage parasite cells (BSs) ranging from 2,500,000 to 25,000. Additionally, mock-infected fish were included as a control group.

Following infection, we measured changes in peripheral blood composition, focusing on expansion of the B cell compartment which is a hallmark of the infection and B cell activation (Figures 1, 2A) (26). Control fish that were mock-infected varied little throughout the experiment and little at early timepoints relative to the non-IS groups. When compared to this mock-infected group, the three IS groups were completely depleted of IgM^+ B cells (Figures 1B, 2A, Supplementary Figure S1). Lymphopoiesis only recovered and produced homeostatic B cell counts on day 41 post-infection in some groups and some individuals (Figure 2A). In contrast, the immunosufficient group had circulating B cells and this compartment began expanding as early as day 21 post-*S. molnari* infection. At this point, the number of peripheral blood IgM^+ B cells increased gradually starting with the group that received the highest dose of 2,500,000 parasites followed by the group receiving ten times less, until IgM^+ B cell counts were four-fold that of the control group on day 41 in the 6^{th} week of infection, the timepoint when we previously observed a peak of B cell expansion (26). The dose-dependent

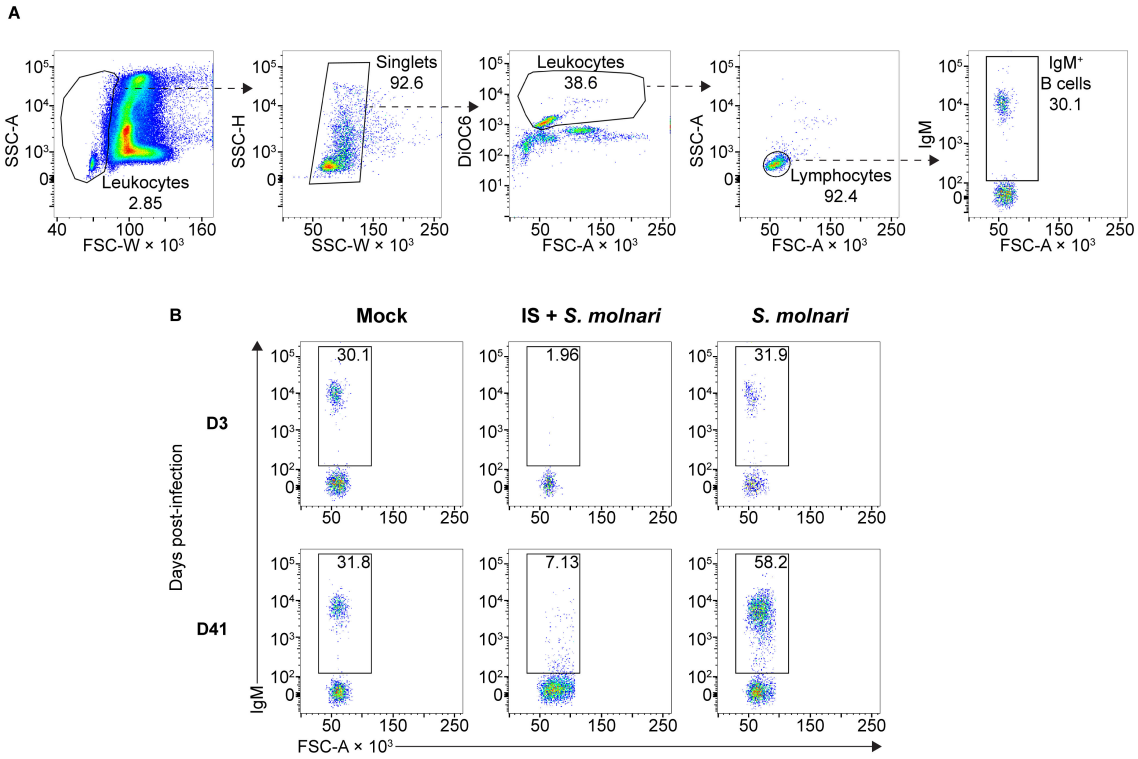

FIGURE 1
The circulating IgM$^+$ B cell compartment of the common carp expands upon infection with the myxozoan *S. molnari* or is depleted upon immunosuppression. **(A)** A representative gating strategy for quantifying the IgM$^+$ B cells in the whole blood of common carp. From the leftmost to the rightmost plots, dashed arrows each point out gated subpopulations (labeled with their proportions) being further analyzed in the plot to their right. The oval morphology of fish red blood cells gives them a heterogeneous scatter profile that overlaps with that of leukocytes. To exclude them, we first broadly gated on cells with low forward scatter width (FSC-W, x-axis), representing all leukocytes. Subsequently, doublets were excluded based on disproportionate side scatter (SSC) width (W) and height (H). Cells stained with the mitochondria- and endoplasmic reticulum-specific DiOC6 (y-axis) can distinguish active cells (leukocytes) from relatively inactive cells (red blood cells) with lower mitochondria or endoplasmic reticulum content. Among the leukocytes, the FSC^{low} SSC^{low} population represents lymphocytes which include IgM$^+$ B cells based on staining with the monoclonal anti-carp IgM antibody WCI12 (mean fluorescence intensity, y-axis of the rightmost plot). Through this strategy, **(B)** we quantified the number of IgM$^+$ B cells (gate and proportions indicated) throughout the experiment: from an early timepoint (day 3, top row) to a late timepoint (day 41, bottom row). Each column represents separate experimental groups either infected with 2,500,000 parasites (*S. molnari*), immunosuppressed and infected with an inoculum of 2,500,000 parasites (IS + *S. molnari*), or mock-infected (Mock). Representative plots are shown.

expansion of the B cells may be a sign of B cell activation and an antigen-specific response. Surprisingly, the blood B cell concentration of the group infected with 25,000 BSs was not significantly different from the mock-infected group (Figure 2A, Supplementary Figure S1).

To measure the B cell response and the outcome of the infection, we quantified antibody titres and parasitemia throughout the experiment. Only baseline non-significantly different anti-*S. molnari* IgM antibodies were detected in the mock-infected and the IS fish (Figure 2B, Supplementary Figure S1). In immunocompetent fish, specific antibody titres were dose-dependent. Curiously, in the group that received the fewest parasites, antigen-specific IgM titres remained at baseline (Figures 2A, B), with a titre comparable to that of the mock-infected and all IS groups (Supplementary Figure S1). We measured an increase in anti-*S. molnari* antibody titres as early as day 28 post-infection in the group receiving the highest dose of parasite (2,500,000 per fish), with the group receiving 10 times fewer parasites following shortly a week later. By the end of the experiment (41 days post-infection), specific antibody titres in these two groups were exponentially higher (<1:1000) than in any other group. Overall, these two groups had comparable anti-*S. molnari* IgM titres but significantly higher titres than any other group (Supplementary Figure S1).

In IS fish, an exponential escalation of the infective dose (between 25,000 to 2,500,000) was matched by an exponential dose-dependent increase in parasitemia (Figure 2C, Supplementary Figure S1). In contrast, the measurements of parasitemia in immunosufficient fish varied in kinetics (e.g., the timepoints at which parasitemia peaks). In these groups, the level of BSs in the blood of immunocompetent fish was ultimately dose-independent unlike in IS groups—parasitemia was not significantly different among these groups (Supplementary Figure S1), and by day 41, all had over 2900-fold less parasitemia than any IS group.

Taken together, our infection model allows us to study the contribution of the B cells to the anti-parasitic response. The immunocompetent fish receiving the lowest dose of 25,000 *S. molnari* had neither increased B cell counts nor increased specific antibody titres (Figures 2A, B). Instead, it is possible that they were protected by non-B cells which helped clear the parasite.

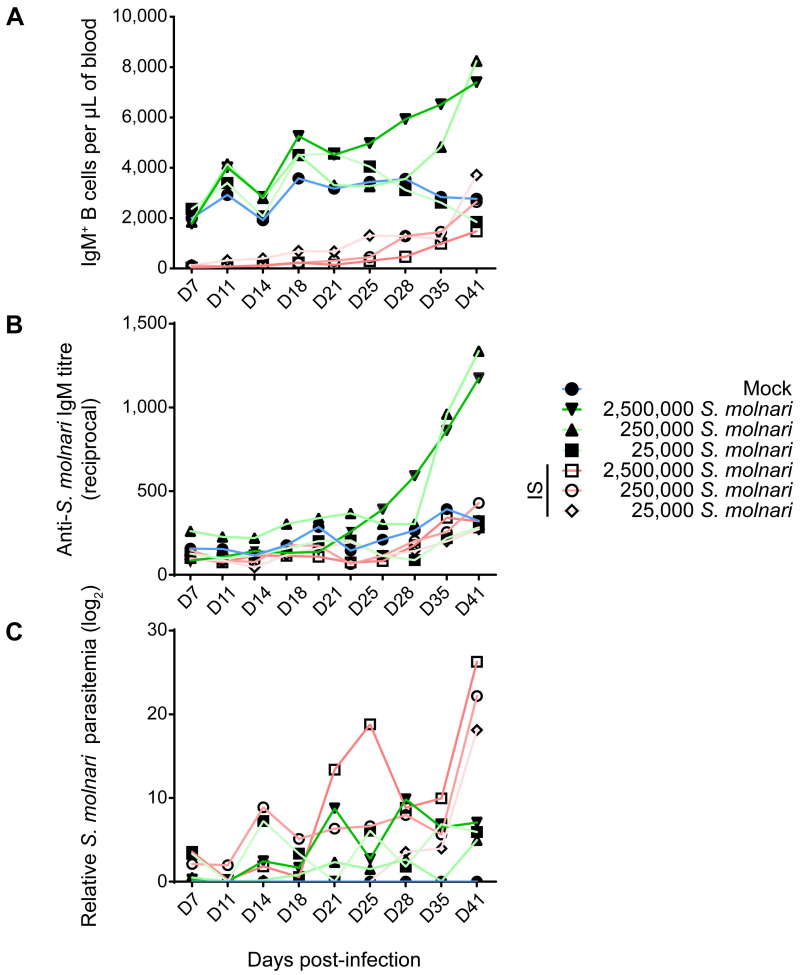

FIGURE 2
Infected common carp produce *S. molnari*-specific IgM which may limit parasitemia. By measuring **(A)** the concentration of peripheral blood IgM$^+$ B cells, **(B)** anti-*S. molnari* IgM antibody titres, and **(C)** parasitemia, we followed the progression of *S. molnari* infection in each of 6 groups of infected fish and one control group, represented by different line colors and symbols (legend on the right). We collected samples and took measurements at the indicated timepoints ranging from 7 to 41 days post-infection (x-axes, D7 to D41). Filled or hollow symbols represent mean measurements from fish that were healthy or immunosuppressed (IS) respectively, at the time of infection; different shades of green or red as well as symbols represent different doses of *S. molnari* used in laboratory infection; the control mock-infected group is represented by blue lines. **(A)** Through the strategy depicted in Figure 1, we quantified the concentration of IgM$^+$ B cells throughout the experiment. **(B)** The unit of measurement presented on the y-axis is reciprocal antibody titre, such that a higher number reflects a higher anti-*S. molnari* titre. **(C)** Parasitemia data was logarithmically transformed and presented in logarithmic units (base 2). n $\geq$ 5 biological replicates per timepoint per group. Please, refer to Supplementary Figure S1 for the statistical analyses.

Overall, we observed that a B cell response requires activation and proliferation, before culminating in antibody secretion. Our data indicate that the immune system of the common carp mounts a protective humoral/B cell response proportional to the parasite inoculum/challenge, with antibodies at least partly suppressing the parasite that would otherwise multiply unchallenged.

2.2 In response to *S. molnari* infection, IgM$^+$ B cells proliferate predominantly in the lymphoid tissue, and express gene signatures of activation and differentiation

We shifted our attention to the splenic and head/anterior kidney lymphoid tissues where B cell responses are initiated. To characterize the B cell response, we measured proliferation and gene expression as indicators of activation and differentiation.

We detected significantly higher proportions of proliferating IgM$^+$ B cells in the blood and head kidney beginning on week 4 (Figure 3). Proliferation uniformly peaked (reached its highest point) and was significantly different from corresponding control groups at week 5 post-infection in all compartments (Figure 3B). This preceded the peak in both blood B cell numbers and antibody titres by a week (Figures 2A, B). EdU incorporation and proliferation returned to baseline in all compartments two weeks later, indicating resolution of acute *S. molnari* infection. As for site specificity, the main compartment of proliferation at week 5 was the head kidney lymphoid organ where over 16% of IgM$^+$ B cells had incorporated EdU versus about 7% in the blood and 8% in the spleen (Figure 3B). Proliferation being predominantly in the head

10.3389/fimmu.2024.1493840

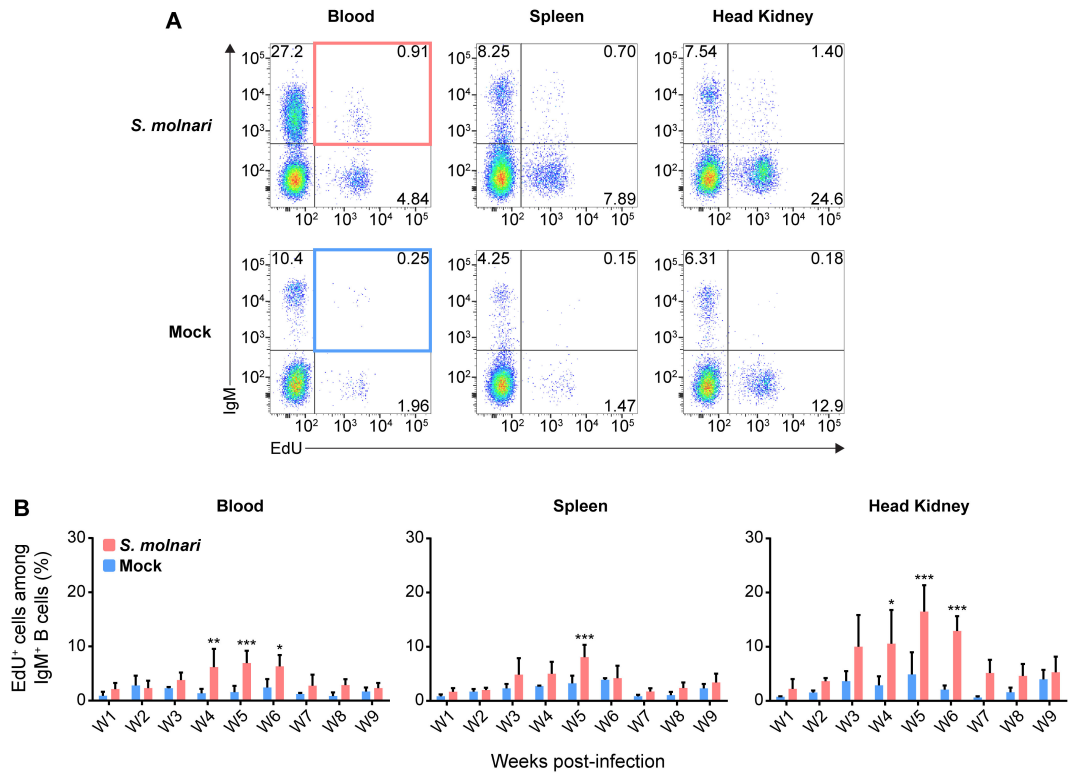

FIGURE 3
Common carp IgM$^+$ B cells proliferate in the blood, the splenic lymphoid organ, and the head kidney lymphoid organ following *S. molnari* infection. **(A)** We exposed fish to the thymidine analogue (EdU) at different time points throughout *S. molnari* infection or in non-infected fish (Mock). As an indicator of proliferation, IgM$^+$ B cells that incorporated EdU were identified by flow cytometry by adapting the gating strategy presented in Figure 1A to detect EdU$^+$ cells in different tissue compartments. Representative plots from week 5 of the infection are presented here, organized by compartment (columns) and fish status (rows). The top two quadrants in every plot are the IgM$^+$ B cell populations of interest. In the first column, the top right quadrants are marked by red or blue quadrilaterals which are the gates we used to quantify IgM$^+$ EdU$^+$ B cells from *S. molnari*-infected or control fish, respectively. **(B)** The proportion of IgM$^+$ EdU$^+$ B cells among total IgM$^+$ B cells was quantified throughout the infection and summarized in bar graphs. Each bar extends to the mean with SD error bars. n = 3 or n = 4 biological replicates per timepoint for the Mock and *S. molnari* groups, respectively. ns (not significant); * $p < 0.05$; ** $p < 0.01$; *** $p < 0.001$.

kidney indicates that it may be a major site of B cell activation and differentiation in *S. molnari* infection.

To uncover and explain the changes that the B cells are undergoing in the head kidney throughout the infection, we profiled gene expression of magnetic-activated cell sorted (MACS-sorted) IgM$^+$ cells (Figure 4A). We selected several predicted orthologues of mammalian and fish markers of B cell differentiation and/or survival (Figure 4B) (13, 34–39). Among the most differentially expressed genes (Figure 4B, top row, over 2-log change in relative gene expression), the significant downregulation of *membIgM* (membrane-bound or cell surface IgM), and upregulation of *secIgM* (secretory IgM), *xbp1*, and *tnfrsf13b* may together indicate differentiation of B cells into antibody-secreting and memory cells (Supplementary Figure S2). Specifically, the peak of *secIgM* and *xbp1* expression at week 5 post-infection corresponds with the timepoint when we began measuring an increase in anti-*S. molnari* IgM titres (Figure 2B) and may be indicative of B cell differentiation into antibody-secreting plasmablasts. The most differentially expressed gene was *tnfrsf13b* which was a significant 6 log units higher than the control group only at week 9 (Supplementary Figure S2). As a receptor in the BAFF/APRIL axis that promotes B cell survival and is also upregulated in rainbow trout by myxozoan infection (38, 39), expression of *tnfrsf13b* (alias *taci*) may indicate the late differentiation of memory B cells. To date, no one has identified an orthologue of the human plasmablast marker *syndecan-1* (alias *cd138*) in teleost fish (40). We measured expression of the related *syndecan-3* but only observed that it was significantly downregulated at weeks 3 and 5. *pax5* and *cxcr5* expression were unchanged but the former trended toward downregulation at late timepoints. Regarding tissue specificity, a two-way ANOVA determined that *secIgM*, *xbp1*, and *tnfrsf13b* expression were significantly higher in the head kidney than in the blood compartment. *Post hoc* testing determined that *secIgM* (at weeks 5, 7, and 9) and *xbp1* (weeks 7, and 9) were significantly overexpressed in the head kidney but not the blood (Supplementary Figure S2). These late-stage and lymphoid organ-specific changes may indicate that *secIgM* and *xbp1* are markers of B cell differentiation in the head kidney.

We further characterized these specimens via multiplex qPCR by profiling expression of B cell markers that were identified by Pan et al.

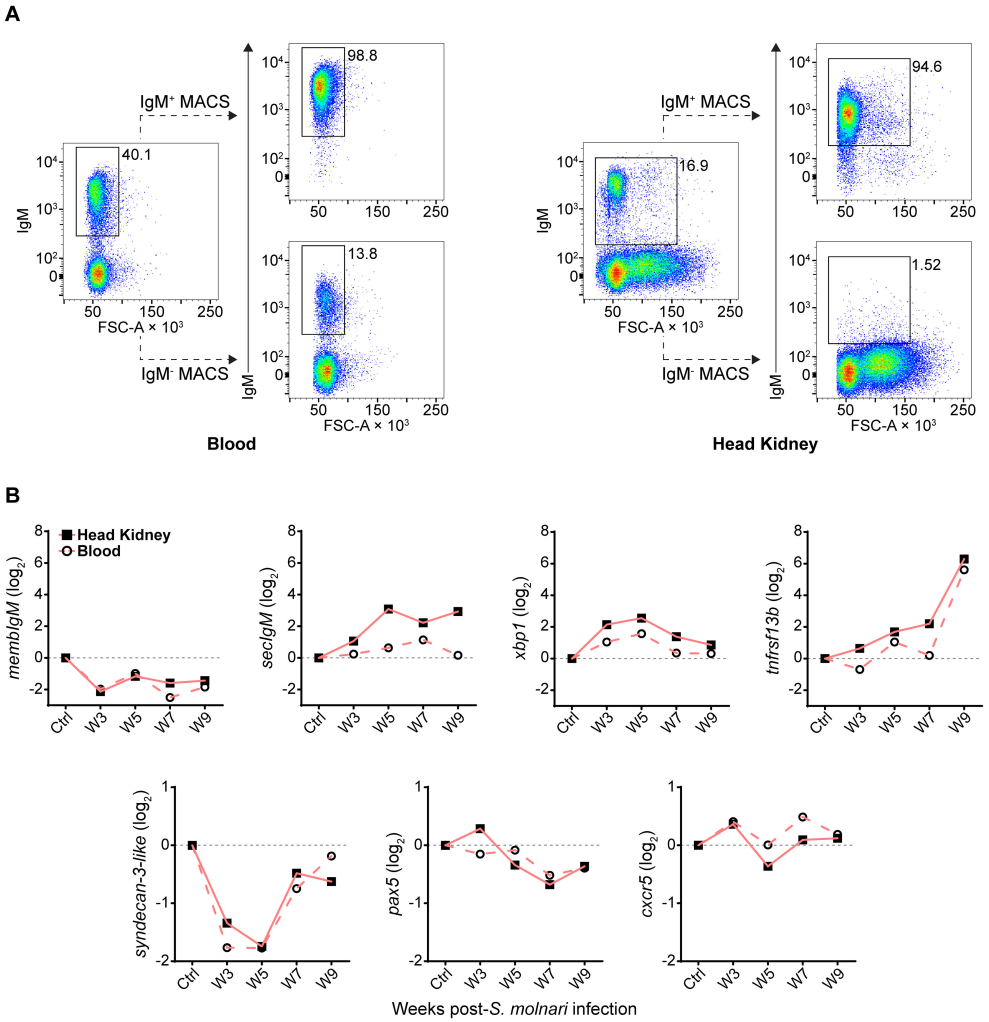

FIGURE 4
Following *S. molnari* infection, common carp IgM$^+$ B cells express markers of B cell activation and differentiation in the blood and head kidney. **(A)** Head kidney or blood IgM$^+$ B cells were MACS-sorted using the monoclonal anti-carp IgM antibody WCI12. Here are two representative MACS results for the blood (left) and the head kidney (right). In each plot, the proportion of IgM$^+$ B cells is adjacent to the corresponding flow cytometry gate. The dashed lines point to the result of MACS: either the eluted IgM$^+$ fraction (IgM$^+$ MACS) or the unbound/washed negative fraction (IgM$^-$ MACS). All plots depict the mean fluorescence intensity of WCI12 staining (y-axes) versus forward scatter area (FSC-A, x-axes). **(B)** RNA from MACS-enriched IgM$^+$ B cells was used to quantify expression of select markers of activation and differentiation throughout *S. molnari* infection. Logarithmically transformed (base 2) relative expression ($2^{-\Delta\Delta CT}$ method) of each marker (y-axes titles) is presented in each plot and organized by highly or weakly differentially expressed genes: respectively, markers in the top row (over 2-log maximum change) or bottom row (under 2-log change). The control group (Ctrl) includes data collected from fish sampled prior to infection. We plotted the mean of relative expression of each group at each timepoint represented by either filled squares connected by lines (head kidney compartment) or hollow circles connected by dashed lines (blood compartment). n ≥ 4 biological replicates per group per timepoint. Please refer to Supplementary Figure S2 for statistical analyses.

in *Ctenopharyngodon idella* grass carp, another cyprinid species (16). Specifically, they are transcripts the authors identified via single-cell RNA sequencing of sorted head kidney IgM$^+$ B cells. Here we present the expression levels of their potential *Cyprinus carpio* orthologues in our MACS-sorted IgM$^+$ B cells (Figure 5). Expression of the 18 genes were hierarchically clustered within the three different compartments throughout the 10-week experiment for comparison between the blood, spleen, and head kidney compartments (Supplementary Figure S3).

The genes were categorized by their annotation and expected roles according to Pan et al.'s single-cell RNA sequencing data (16), and/or the cell population they help identify (Figure 5). The expression of *cd83*, *cxcr4b*, *egr1*, *klf2a*, and *ier2* were significantly different compared to the non-infected control group and the results of *post hoc* multiple comparisons tests are summarized in Supplementary Figure S4. Notably, three of them are activation markers. *klf2a*, and *egr1* were downregulated at early timepoints (specifically, week 2 post-infection); *egr1* was later upregulated between week 5 and 8 preferentially in the lymphoid organs while upregulation of *klf2a* was delayed and centered around week 8 (Supplementary Figure S4). Among the co-stimulatory molecules, *cd83* was significantly overexpressed relative to the control group in all compartments and throughout the experiment with the exception of the week 5 and week 6 timepoint (Figure 5, Supplementary Figure S4) unlike *cd86* which peaked at week 1 in

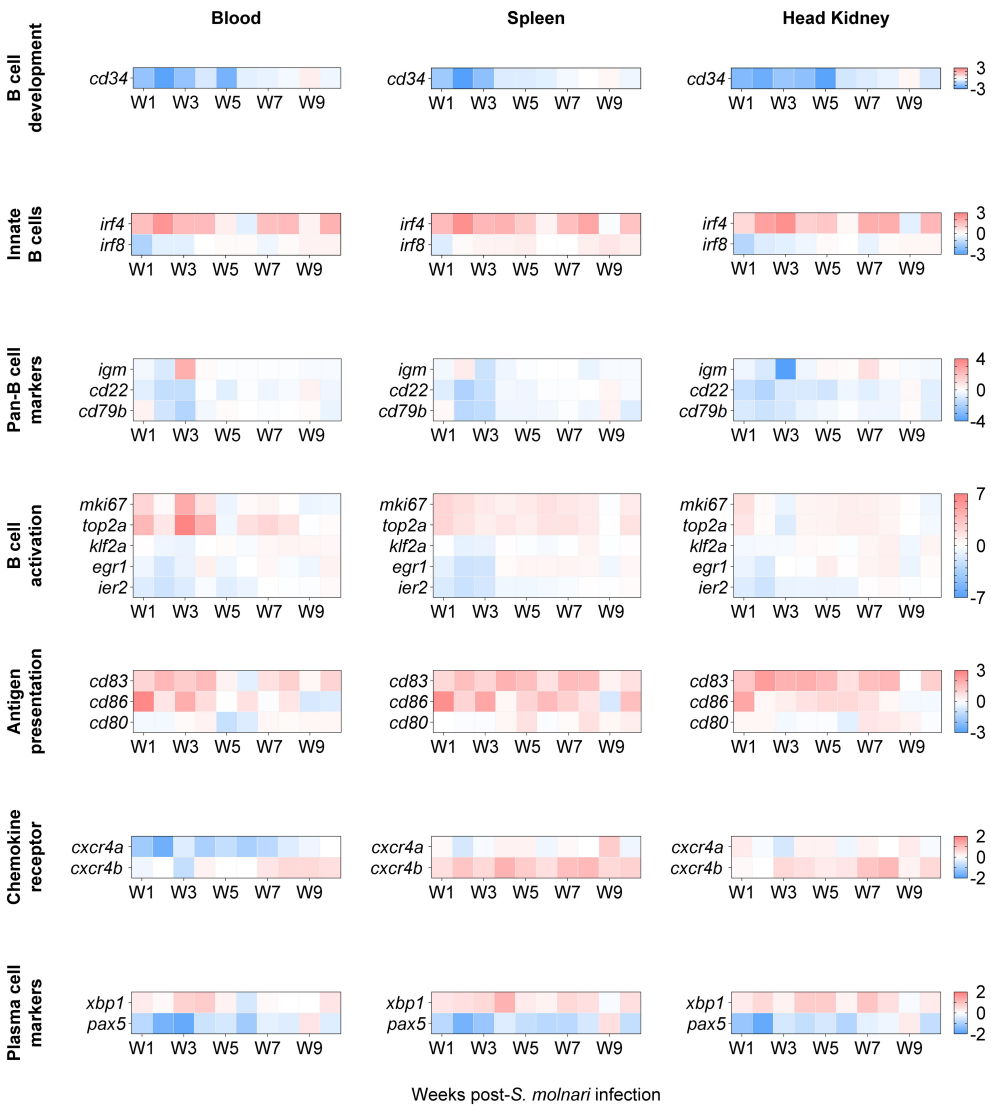

FIGURE 5
The transcription profile of cyprinid markers of developing, innate, activated/proliferating, antigen-presenting, and differentiated IgM$^+$ B cell subpopulations. We profiled expression of markers defining distinct B cell subpopulations, i.e. genes initially identified in single-cell RNA sequencing analysis of grass carp IgM$^+$ B cells (16). Here, genes were categorized (in separate rows of heat maps) based on the subpopulations they cluster, by developmental stage, and/or by activities such as activation and antigen presentation. The two-color gradient represents either overexpression or downregulation relative to the control group (not shown here). The legends for each gene category are on the rightmost side of each set of heat maps. Data in absolute number of copies of each gene were normalized to the number of copies detected in the control group and then logarithmically transformed (base 2) to better reflect both positive and negative fold changes. n ≥ 4 biological replicates per gene per timepoint. For statistical analyses, please refer to Supplementary Figure S4.

all three compartments. Relative to the non-infected control group, *cxcr4b* was overexpressed at almost all timepoints between week 2 and week 10 in the splenic and head kidney lymphoid organs (Figure 5, Supplementary Figure S4). *cxcr4b* may be the functional carp orthologue for retaining or directing select B cells to lymphoid tissues unlike *cxcr4a* (Figure 5) and *cxcr5* (Figure 4).

A notable difference with Pan et al.'s study (16) is that we are studying these markers at the population level (in bulk) rather than at the level of single cells. Therefore, we still expect changes in subpopulations of IgM$^+$ B cells and changes in B cell marker expression even if these are more difficult to detect and not statistically significant. Among the markers whose expression was not significantly different from the control group, *cd34* is a marker of mouse and human hematopoietic stem cells. *cd34* expression was downregulated relative to the control group in all compartments during the first 5 weeks of infection (Figure 5). Two markers of innate B cells, *irf4* and *irf8*, trended oppositely with the former highly overexpressed and the latter downregulated at early timepoints in all compartments. Among the pan-B cell markers, the most notable change was a 2.5-log upregulation and a 4-log downregulation of *igm* compared to their controls in the blood and head kidney, respectively, at the same week 3 timepoint. Similarly, the expression patterns of the activation markers *mki67* and *top2a* matched those of *igm* in the same cellular compartments at the same week 3 timepoint, suggesting

that all three may be markers of the same IgM$^+$ cell subpopulation. Finally, we again observed a reverse pattern of *xbp1* and *pax5* expression which is an indicator of an ongoing immune response and B cell differentiation (Figures 4, 5).

In summary, considering that all these markers define distinct cyprinid IgM$^+$ B cell subpopulations (16), our results suggest that there is: reduced hematopoiesis or lymphopoiesis; activation of an innate B cell population; antigen-presenting cell (APC) activity or costimulation; activation, proliferation, and differentiation of B cells; migration/retention of cells in lymphoid tissues. Together, these changes may be the origin of the humoral response against the parasite (Figure 2).

2.3 Memory B cells are produced throughout the acute response to *S. molnari* and persist as resting cells

Fish that survive a primary myxozoan infection presumably harbor memory lymphocytes that protect them from secondary infections. We gathered evidence that the initial immune response produces a greater breadth of B cells than we could previously appreciate with anti-carp IgM staining alone. Yet, we could not directly identify memory cells as there is so far no marker for let alone a defined subpopulation of teleost memory B cells. Furthermore, we must study these cells on the order or scale of months that are most relevant to immunological memory, vaccine success, and protection from natural seasonal (re-)infections.

We revisited the EdU pulse labeling method, and searched for EdU$^+$ IgM$^+$ B cells months after infection which should theoretically reveal B cells that were i) activated upon encountering *S. molnari* (antigen), ii) proliferated and incorporated EdU as a result, and iii) differentiated into long-lived quiescent cells that retain the EdU. The latter are selected into the memory pool following the contraction and resolution phases of the primary immune response. To test this, we assigned fish to six labeling windows/groups receiving EdU during a specific week following acute *S. molnari* infection. Approximately six months after infection and approximately five months following EdU injection, we detected EdU$^+$ cells in the blood, spleen, and head kidney compartments (Figures 6A, B).

Astonishingly, EdU$^+$ IgM$^+$ B cells were readily detectable in the lymphocyte gate, representing around 2% to 5% of all IgM$^+$ B cells (Figures 6A, B) and potentially include memory cells. In contrast, a negligible amount of weakly EdU$^+$ cells were detected among granulocytes from the same fish (Figure 6A). Compared to proliferation during the acute infection (Figure 3), the distribution of EdU$^+$ cells was mainly in the blood and spleen rather than the head kidney, which matches the location of the resting B cells described by Ma et al. (13); interestingly, they were not labeled during the 5th week of acute infection, and peak proliferation (Figures 3, 6C). The majority of EdU$^+$ IgM$^+$ cells originated from week 7 post-infection and at the time of measurement, represented 6% of all splenic IgM$^+$ cells, and this number was about 4% and 3% in the peripheral blood and head kidney, respectively.

In other words, out of all the proliferating and EdU-incorporating cells during acute infection, a subset survived, having not been turned over, not proliferated further, and not diluted EdU below the threshold of detection. This B cell population may be partly composed of the fish equivalent of the memory B cell, a non-dividing recirculating B cell subset awaiting reactivation.

2.4 A head kidney-exclusive B cell subpopulation with high levels of intracellular IgM may represent plasma cells

Plasma cells and their antibody effector molecules make up another pillar or wall of humoral memory. We were able to detect anti-*S. molnari* antibodies eight months post-infection, long after resolution of parasite infection and without any reinfection or immunization (Figure 7A). With these antibodies being presumably produced by plasma cells, we devised methods to detect this B cell subset based on the exceptional amounts of Ig they produce, their levels of membrane IgM (memb IgM) (36), their size, their compartmentalization in the head kidney (13), and hypothesized resistance to hormonal stress (41).

Thus, we costained cells in a step-wise manner to detect the extracellular membrane IgM (Memb IgM) and intracellular IgM (IC IgM) using a single monoclonal anti-carp IgM antibody. In the blood and spleen, the B cells stained minimally for IC IgM with a slight upward shift of the BCR^{high} population of cells (Figure 7B, top row). This did not reveal any new population among the cells we have always detected (Figure 1). However, the head kidney revealed two new B cell populations that were previously undetectable through Memb IgM staining alone (Figure 7B, top row): a Memb IgM$^-$ IC IgM^{mid} population and a Memb IgM^{mid} IC IgM^{high} population. The former is relatively abundant (representing around 3% of all leukocytes) while the latter is exceedingly rare (representing around 0.5% of all leukocytes). Overall, based on their phenotype and tissue-specificity, we hypothesized that one of these populations represents plasma cells.

To test these cells' resistance to stress, we immunosuppressed fish that had previously been infected with *S. molnari*. As corticosteroid-induced immunosuppression targets lymphopoiesis (42), dividing cells, and short-lived cells, we hypothesized that plasma cells would be resistant and would not be depleted unlike their naïve B cell counterparts. This treatment eliminates virtually all IgM$^+$ B cells from the blood (Figures 1B, 2A). In the spleen and head kidney, this approach depleted the most abundant B cell populations including the Memb IgM$^-$ B cell population (Figure 7B, bottom row). In contrast, the Memb IgM^{mid} IC IgM^{high} population became readily detectable in the head kidney (over 2% of all leukocytes in the example). We also hypothesized that they would continue producing antibodies despite the immunosuppression and were responsible for keeping the parasite latent long-term. Thus, we measured antibody titres and parasitemia in the weeks following immunosuppression (Figure 7A). Anti-*S. molnari* IgM antibody titres doubled and coincided with the reemergence of the parasite

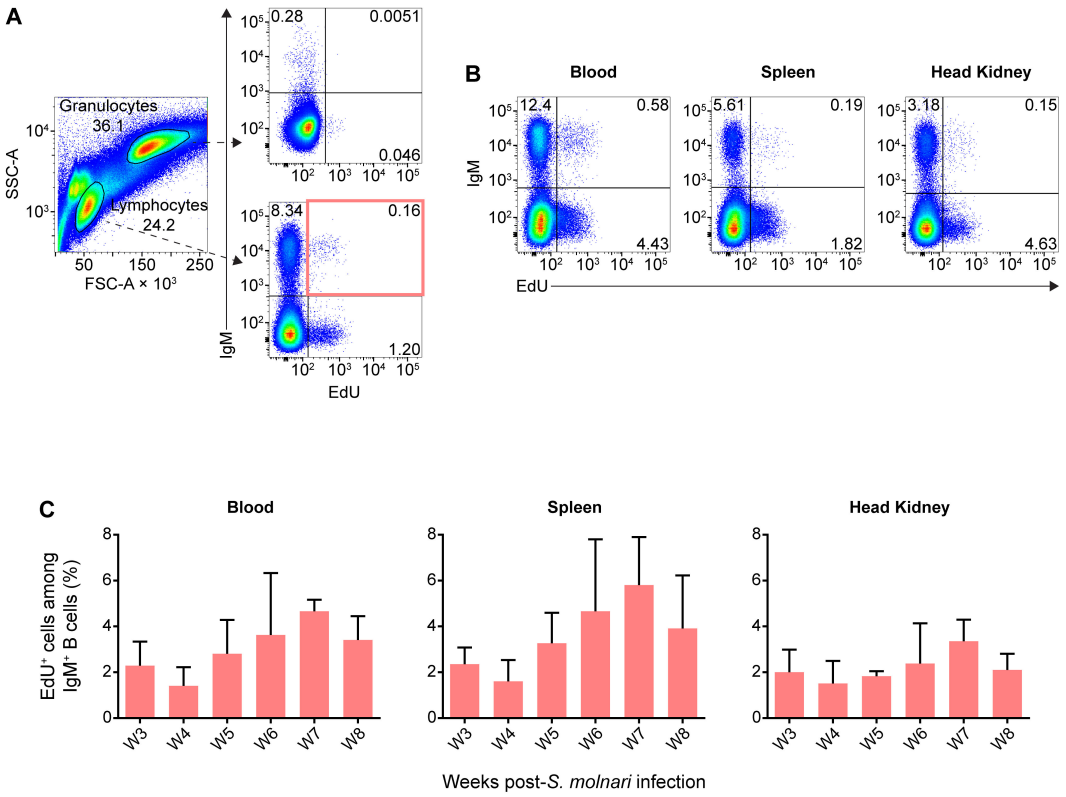

FIGURE 6
IgM$^+$ B cells proliferating during acute *S. molnari* infection persist over five months later as resting cells. **(A)** In flow cytometry analysis of representative common carp head kidney leukocytes (left plot), distinct side scatter area (SSC-A, y-axis) and forward scatter area (FSC-A, x-axis) profiles help distinguish granulocytes (FSC-A^{high} SSC-A^{high}) from lymphocytes (FSC-A^{low} SSC-A^{low}). As indicated by dashed arrows, these two leukocyte populations were subsequently analyzed for/categorized by IgM expression (y-axis) and intensity of incorporated EdU (x-axis). Despite the months-long gap between EdU labeling and detection instead of next-day detection (Figure 3), EdU$^+$ subpopulations were readily detectable among lymphocytes (bottom right plot), but rare among granulocytes (top right plot). **(B)** Additional examples of EdU$^+$ IgM$^+$ lymphocytes from the blood, spleen, and head kidney are presented. Proportions of each quadrant/subpopulation are noted on plots. In **(A)** we highlighted the main EdU$^+$ IgM$^+$ population of interest via a red rectangle and the proportion of this subpopulation relative to total IgM$^+$ lymphocytes is summarized in bar graphs in **(C)**. These graphs are organized along the x-axes by separate bars (mean + SD), each representing a labeling window: the week post-*S. molnari* infection in which each group was injected with EdU. Representative data presented from the week 4 and 7 labeling windows in **(A, B)**, respectively. n ≥ 3 biological replicates.

and an over 10-log increase in parasitemia at the final timepoint of 41 days post-immunosuppression.

Together, our data indicate that the initial B cell response (Figures 1, 2) elicits constitutive antigen-specific antibody production. The source of these antibodies may be the corticosteroid-resistant, head kidney-resident, IC IgM^{high} B cell population, which are significantly larger and denser than their counterparts with high Memb IgM expression (Figure 7C). These cells and antibodies may be one component of constitutive defense keeping *S. molnari* latent and/or protecting the host from future infections.

3 Discussion

Overall, our data indicate that B cell activation follows a similar course to that in 'higher' vertebrates and produces specialized cellular subsets with memory and (constitutive) antibody-secreting phenotypes, together forming 'two walls of protection' (43). Our results indicate that the initial B cell response is protective and prevents the worst form of disease caused by *S. molnari* (the only two deaths recorded in this experiment were from the IS groups).

3.1 The B cell response, memory B and plasma cells in a teleost fish

In mammals, antigen activates B cells and they differentiate in lymphoid tissues. This process can be divided into at least two phases: an initial phase that produces the short-lived plasmablasts and some memory B cells, whereas a second phase produces memory B and long-lived plasma cells that have affinity-matured and have been positively selected for in germinal center reactions (44, 45).

The B cell response we observed was dose-dependent, and antigen-specific. In comparison to the response of rainbow trout to the model hapten-protein antigen TNP-KLH, anti-*S. molnari* antibody production was accelerated, and titres were exponentially higher at the same timepoint (12). The initial surge in antibody

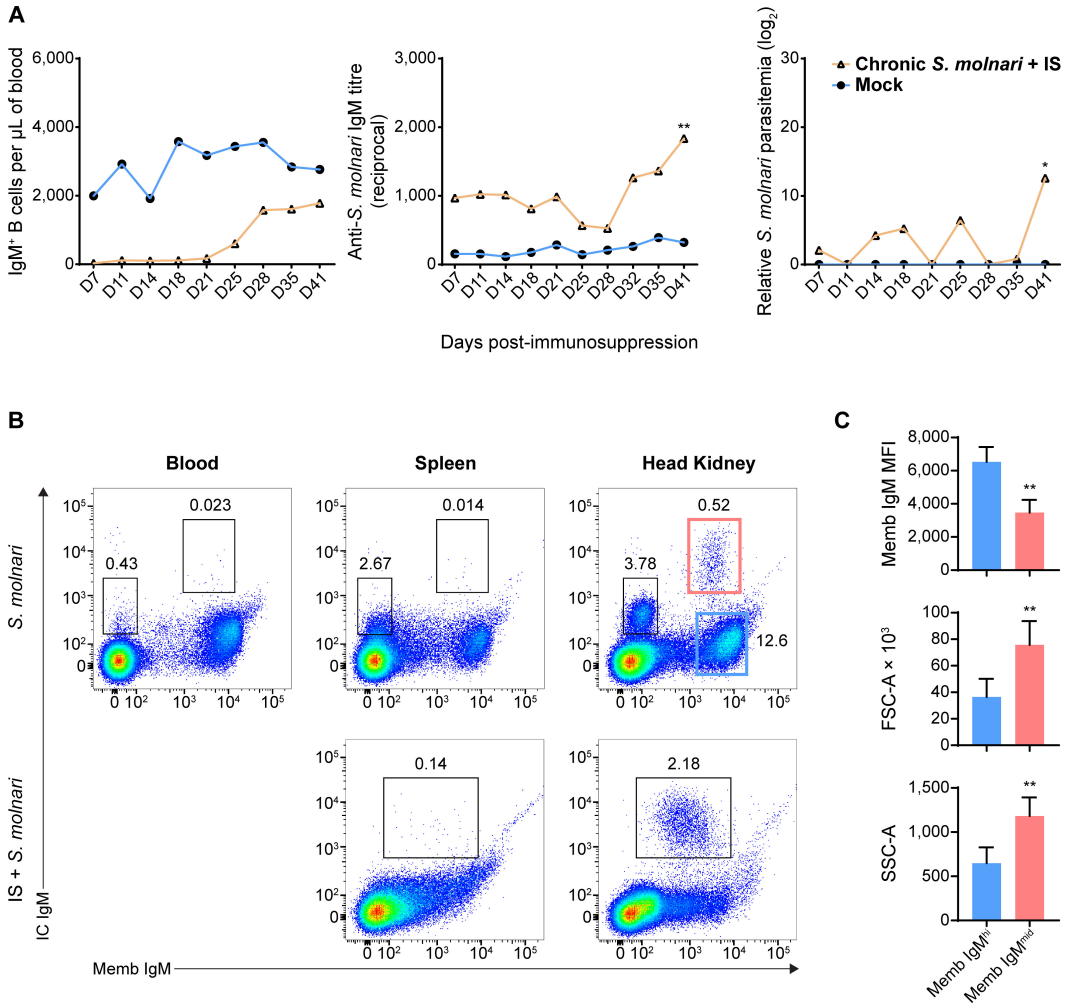

FIGURE 7
A population of head kidney-specific large B cells with exceptionally high levels of intracellular IgM and resistance to immunosuppression may represent plasma cells of the common carp. **(A)** We studied a cohort of immunocompetent carp infected eight months prior which have not achieved sterile immunity (labeled 'Chronic *S. molnari*'). Unlike fish infected for the first time (Figure 1, the 'Mock' control group was sampled simultaneously as the 'Chronic *S. molnari*' group), these carp constitutively produced anti-*S. molnari* IgM (middle plot) which are conventionally produced by plasma cells. As we hypothesized that plasma cells are resistant to immunosuppression, the 'Chronic *S. molnari*' cohort of fish was treated with triamcinolone acetonide (IS) which did not decrease specific antibody titres throughout the experiment despite completely depleting circulating IgM^+ B cells (left plot). Nonetheless, parasitemia (right plot) was measurable in these fish. Orange line and triangle symbols represent the 'Chronic *S. molnari* + IS' group whereas the blue line and circles represent an uninfected control cohort mock-infected (Mock). We performed immunosuppression on day 0 and thus the x-axis represents the days post-immunosuppression or -mock injection. **(B)** We identified a population of putative plasma cells via costaining for membrane/cell surface IgM (memb IgM, x-axes) and intracellular IgM (IC IgM, y-axes) lymphocytes. This IC IgM^{high} population was detectable exclusively in the head kidney (rightmost column). Despite near-complete depletion of IgM^+ B cells in the blood (Figures 1B, 2A), and head kidney, triamcinolone acetonide treatment (IS) enriched this IC IgM^{high} population in the head kidney (bottom right plot). **(C)** Each bar indicates the mean of either the mean fluorescence intensity (MFI) of membrane IgM staining, forward scatter area (FSC-A), or side scatter area (SSC-A) + SD. For these metrics, statistically significant differences between the memb IgM^{high} and memb IgM^{mid} populations, respectively outlined in blue and red rectangles in **(B)**, were determined by the Wilcoxon signed rank test with the two populations as matched pairs in n = 8 biological replicates. * $p < 0.05$; ** $p < 0.01$.

production at the 5-week timepoint (Figure 2B) is likely the product of short-lived plasma cells or plasmablasts and matches the timing of the significant increase in *igm* transcripts we previously observed in the same model and in this study (Figures 4, 5) (26).

We measured a peak of proliferation at week 5 post-infection and detected a significant proportion of EdU^+ IgM^+ B cells in both the head kidney and spleen. These cells likely include those described in a recent report by Shibasaki et al. of a germinal center analogue in the rainbow trout spleen (33). By detecting highly proliferating B and T cells adjacent to melanomacrophages, Shibasaki et al. convincingly identified sites that support clonal expansion, antigen receptor affinity maturation, and clonal selection. One expected output is antibody-secreting cells which circulate and contribute to the sharp rise in the number of IgM^+ and EdU^+ B cells at week 5 and 6 in the blood even though it is not a site of proliferation (Figures 2A, 3). The short-term distribution of antibody-secreting cells throughout the periphery was also observed by Davidson et al. in *Limanda limanda* following immunization

with human gamma globulin (11). The precise identity of the circulating B cells can be confirmed with a strategy like the one we used to detect the kidney-resident IC IgM^{high} cells. However, they are only expected to be short-lived and provide short-term protection.

Regardless of which phenotypic markers they express, regardless of species-to-species variations, the purest and most universal definition of what is a memory B cell is their longevity. We traced the proliferating cells of the primary response to determine if they persist long after resolution of the acute response. We hypothesize that the EdU^+ cells we detected months after infection/labeling include clones that avoided caspase-mediated apoptosis in the melanomacrophage centers (33). The upregulation of *secIgM*, *xbp1*, *tnfrsf13b*, and downregulation of *membIgM*, and *pax5* may also be byproducts of ongoing selection and differentiation. We detected memory B cells in every compartment, and they formed at every timepoint studied. The memory B cells detected in the spleen and blood matches where Ma et al. observed them in rainbow trout (13). These cells are likely recirculating between the two compartments, explaining why their proportions are very similar in the two compartments. In contrast, the head kidney of carp and other bony fish species appears to be a niche for plasma cells that do not recirculate. These cells likely reside in the head kidney which is a survival niche for plasma cells of other bony fish species as well (13, 14, 16, 46).

The emergence of memory cells and the peak of their formation in week 7 (Figure 6C) was relatively late and did not correlate with the peak of B cell proliferation in week 5 (Figures 2B, 3). Considering the timing and selection mechanisms ongoing in lymphoid tissues, it is likely that early memory B cells express low affinity BCRs and this affinity gradually matures as observed in rainbow trout and channel catfish (12, 13, 15) driven by activation-induced cytidine deaminase-mediated antigen receptor diversification in germinal center analogues (33). In our study, we hypothesize that the late-stage memory cells emerging in week 7 may be successful progenitors of melanomacrophage center reactions, and express affinity-matured BCRs which confer a survival/fitness advantage.

3.2 Humoral memory and the implications for vaccination and natural immunity

In humans, there is evidence that exposure to a pathogen is sufficient to protect an individual for a lifetime: in a 2008 study, survivors of the 1918 H1N1 influenza pandemic continued to harbor memory cells producing strain-specific anti-hemagglutinin neutralizing antibodies, nearly 90 years after exposure to the virus (47). If fish B cells behave in much the same way, there are major implications for vaccination and natural acquired immunity against pathogens. In a study similar to ours in mice, memory B and plasma cell retained BrdU at the 8-week timepoint (48). Here, we continued to detect EdU^+, IgM^+ B cells well after 6 months post-infection and EdU pulse labeling. A recent Atlantic salmon vaccine trial demonstrated persistent antigen-specific antibody titres over 80 weeks post-immunization, in a full aquaculture production cycle (18). Gilthead seabream that had survived a previous infection with the myxozoan *Enteromyxum leei* maintained specific antibody titres for over 16 months (17). This progress and such milestones are consequential because we need to know how long memory is maintained post-vaccination or whether fish having already survived an initial infection will be immune during next year's outbreak. Understanding how this memory is generated and maintained will help us move away from purely empirical vaccines and methods, and towards conferring acquired immunity.

Existing models propose that memory B cells could be maintained by continuous antigen exposure while others propose that their longevity may be intrinsic to 'tonic' BCR signaling (44). The aforementioned Atlantic salmon vaccine trial demonstrated retention of select antigens many months post-vaccination in granulomas forming in the pancreas but not in lymphoid organs (18). Alternatively, B cells could also be re-exposed to antigen via booster immunizations to provide survival signals and maintain antibody titres (44). Considering the discovery of a germinal center analogue in fish (33), the fish memory B cells we detected may potentially also re-enter melanomacrophage centers to further diversify their antibody repertoire and/or differentiate into (short-lived) plasma cells, providing a 'faster' and 'stronger' secondary immune response as occurs in mammals (44).

Finally, we do not know if the survival of memory cells in laboratory settings would be reproducible in natural settings where animals are exposed to environmental stressors. At least in Atlantic salmon in a farm setting, specific antibody titres were maintained over 80 weeks post-immunization despite the seasonal changes in temperature and photoperiod (18). In our study, we mimicked the effects of stress-induced cortisol/glucocorticoids in *S. molnari*-infected fish. Abnormally high stress-induced plasma cortisol increases the susceptibility of trout to fungal and bacterial infection (49). In our study, after administration of the corticosteroid, antibody titres remained stable (Figure 7A) without *de novo* B cell lymphopoiesis (44), without circulating naïve B cells, and without *de novo* antibody production, despite the half-life of fish IgM being reportedly mere days (50). Thus, it suggests that anti-*S. molnari* plasma cells would survive such a stressor and that their antibody production is not affected (Figure 7B). The resistance of plasma cells may also be non-hormonal as observed in rainbow trout plasma cells resistant to hydroxyurea (14). The overall resilience of plasma cells may make them key to long-term protection that supports, for example, the physiology and life cycle of spawning fish as hypothesized by Zwollo (41). In this 'immunological imprinting' scenario, plasma cells are generated in juvenile fish against pathogens in their rearing site. As adults returning to these sites during their 'spawning journey', Zwollo hypothesizes that plasma cells may be resistant to cortisol, have a survival advantage over other B cell populations, and continue producing antibodies in anticipation of familiar pathogens (41).

Mechanistically, fish splenic and kidney leukocytes express glucocorticoid receptors (51) and cortisol induces apoptosis of *C. carpio* peripheral blood leukocytes (52). In addition to higher bacterial disease susceptibility (49), another study using triamcinolone acetonide demonstrated that it can nullify immune protection and perhaps memory of *C. carpio* against the protozoan parasite *Ichthyophthirius multifiliis* via an unknown mechanism

(31). Interestingly, the same authors measured unchanged specific antibody titres following administration of the drug (30).

3.3 Potential lessons from the *S. molnari* infection model

Chronic infections pose the greatest challenges even in well-studied species. For example, despite decades of concentrated research efforts, there is still no vaccine available against pathogens causing chronic diseases such as human immunodeficiency virus and malaria. Interestingly, in malaria infection, despite robust production of plasmablasts and anti-*Plasmodium* antibodies, this was ultimately metabolically taxing and impaired production of memory B and plasma cells (53). Our data suggests that we can rule out this possibility to explain chronic *S. molnari* infection because we measured a persistent constitutive anti-*S. molnari* response.

In natural settings, could immunosuppression (e.g., via cortisol) be a trigger for parasite activation, spore formation, and perpetuating the life cycle? Sterilizing immunity to myxozoan infections is rare and fish become carriers, suggesting that the parasite can evade the immune system, potentially a general feature of myxozoans that have co-evolved with fish hosts (54, 55). Despite continued secretion of anti-*S. molnari* antibodies, humoral memory could not provide sterilizing immunity in chronically infected fish (Figure 7A). Even though the immune antisera of infected fish can lyse the parasite (manuscript in preparation), the latent parasite was able to re-emerge 41 days after administration of the corticosteroid. It is possible that plasma cells expressing antibodies specific to an original 'founder' variant could no longer recognize an escape variant of the parasite, or that other immune non-B cells are protective and also eliminated by the corticosteroid we administered, i.e., the B cell response is necessary but insufficient alone. Taken together, myxozoan parasite escape and sporulation may be side effects of the 'immunological imprinting hypothesis' and hormonal immunosuppression (41). In this model, interseasonal carriers such as the common carp or wild trout may spawn and produce invertebrate-infective spores. Infected invertebrates may produce the fish-infective spores, completing the parasite life cycle and causing the annual outbreaks of myxozoan infections.

3.4 Concluding remarks

In summary, we adapted and devised methods that may be applicable to other vertebrate species in which adaptive immunity and immunological memory can be demonstrated because it relies on a common phenomenon, not a common mechanism or marker. Perhaps what holds true for all vertebrates and the only all-encompassing definition is that memory lymphocytes are antigen-experienced after engaging in a past immune response, and persist after resolution of that response. Immunologists have observed immunological memory for over a century and achieving humoral memory will help us meet the needs of immunologists, parasitologists, and fish husbandry.

4 Materials and methods

4.1 Key resources table

Please refer to Table 1 for the key resources used in this study.

4.2 Experimental model details

Animal procedures were performed in accordance with Czech legislation (section 29 of Act No. 246/1992 Coll. on Protection of animals against cruelty, as amended by Act No. 77/2004 Coll.). Animal handling complied with the relevant European guidelines on animal welfare (Directive 2010/63/EU on the protection of animals used for scientific purposes) and the recommendations of the Federation of Laboratory Animal Science Associations. The animal experiments were approved by the Ministry of Education. Approval ID: MSMT-4186/2018-2. Our study is reported in accordance with ARRIVE guidelines (https://arriveguidelines.org).

We reared specific pathogen-free (SPF) common carp (*Cyprinus carpio*) from peroxide-treated fertilized eggs (700 mg/L for 15 min) in an experimental recirculating system in the animal facility of the Institute of Parasitology, Biology Centre CAS. During the experiment, fish with an average mass of approximately 25 g were selected and fed twice a day with a commercial carp diet (Skretting) at a daily rate of 1.5% of their body mass. The sex of experimental fish was not considered in our study. The fish were implanted with passive integrated transponders to track the experimental group they belonged to. We housed fish randomly and therefore fish from different experimental groups shared the same tanks. However, all tanks shared the same water which was UV-irradiated, ozonized water at 21 ± 1°C, with water quality (oxygen, pH, ammonia, nitrite and nitrates) monitored daily using probes and titration tests. Ammonia levels never surpassed 0.02 mg/L.

4.3 Experimental infections and fish

For all infections, we collected *S. molnari* parasite from the fish host and purified the BSs via DEAE cellulose (BIOpHORETICS, Sparks, NV, USA) isolation as described previously (19).

For the trial measuring B cell counts, antibody titres, and parasitemia, fish were divided into eight groups of six fish each for the initial kinetic measurements of peripheral blood concentration, antibody titres, and parasitemia: groups 1-3 were immunocompetent/immunosufficient and received one of three ten-fold diluted doses of parasite ranging from 2,500,000 to 25,000; groups 4-6 were also given one of the three doses of parasite as described for groups 1-3 but these fish were immunosuppressed with triamcinolone acetonide (Glentham Life Sciences, Corsam, UK) at a dose of 200 µg/g of body mass the day before intraperitoneal injection of the parasite (19, 30–32, 56); finally, one group was mock-infected via injection of sterile Roswell Park Memorial Institute 1640 medium in the same site (RPMI 1640, Life Technologies Limited, Paisley, UK). RPMI 1640 also served as the medium for *ex vivo* parasite. Fish that were not

10.3389/fimmu.2024.1493840

TABLE 1 Key resources table.

REAGENT or RESOURCE	SOURCE	IDENTIFIER	ADDITIONAL INFORMATION
Antibodies			
Monoclonal antibody supernatant WCI12	Secombes et al., 1983 (57)		Flow cytometry (1:100), ELISA (variable)
Goat Anti-Mouse IgG H&L (APC)	Abcam	Cat#ab130782	Flow cytometry (1:500)
Goat Anti-Mouse IgG Antibody, HRP conjugate	Sigma-Aldrich	Cat#12-349	ELISA (1:5000)
Anti-Mouse IgG MicroBeads	Miltenyi Biotec	Cat#130-048-401	
Biological samples			
Common carp (*Cyprinus carpio*) blood, spleen biopsies, and head kidney biopsies	Laboratory-reared fish from the Institute of Parasitology, Biology Centre, CAS		
Chemicals, peptides, and recombinant proteins			
Triamcinolone acetonide	Glentham Life Sciences	Cat#GP6845	200 µg/g of body mass
DEAE 52 cellulose	BIOpHORETICS	Cat#B45059	
RPMI 1640	Gibco	Cat#A4192301	
3,3′-Dihexyloxacarbocyanine iodide [DiOC6(3)]	Sigma-Aldrich	Cat#318426	
cOmplete Protease Inhibitor Cocktail	Roche Diagnostics	Cat#11697498001	
TMB Substrate Kit	Thermo Fisher Scientific	Cat#34021	
Percoll	Cytiva	Cat#17089101	
Ficoll-Paque PREMIUM	Cytiva	Cat#17544202	
RNAlater Stabilization Solution	Thermo Fisher Scientific	Cat#AM7021	
Exonuclease I (*E. coli*)	New England Biolabs	Cat#M0293	
EZ-Link Sulfo-NHS-LC-Biotin	Thermo Fisher Scientific	Cat#21335	
HBSS, no calcium, no magnesium, no phenol red	Gibco	Cat#14175095	
eBioscience IC Fixation Buffer	Thermo Fisher Scientific	Cat#00-8222-49	
eBioscience Permeabilization Buffer (10X)	Thermo Fisher Scientific	Cat#00-8333-56	
eBioscience Streptavidin PE-Cyanine7 Conjugate	Thermo Fisher Scientific	Cat#25-4317-82	Flow cytometry (1:500)
Commercial assays			
Click-iT EdU Alexa Fluor 488 Flow Cytometry Assay Kit	Thermo Fisher Scientific	Cat#C10420	
NucleoSpin RNA, kit for RNA purification	MACHEREY-NAGEL	Cat#740955	
Power SYBR Green RNA-to-CT 1-Step Kit	Applied Biosystems	Cat#4389986	
Reverse Transcription Master Mix	Standard BioTools	Cat#100-6298	
Preamp Master Mix	Standard BioTools	Cat#100-6298	
SsoFast EvaGreen Supermix	Bio-Rad	Cat#1725200	
Mouse TCS Antibody Purification Kit	Abcam	Cat#ab128749	
Experimental models: Organisms			
Healthy common carp (*Cyprinus carpio*), adults of approximately 25 g	Laboratory-reared from the Institute of Parasitology, Biology Centre, CAS		
Sphaerospora molnari	Wild isolate, lab-propagated at the Institute of Parasitology, Biology Centre, CAS		

(Continued)

TABLE 1 Continued

REAGENT or RESOURCE	SOURCE	IDENTIFIER	ADDITIONAL INFORMATION
Oligonucleotides			
Please, see Supplementary Table S1 for all *Cyprinus carpio*-specific oligonucleotides we designed for this study.			
Software			
BD FACSDiva software	BD Biosciences	https://www.bd.com/	
FlowJo v10	FlowJo LLC, Tree Star	https://www.flowjo.com/	
Prism 10	GraphPad	https://www.graphpad.com/scientific-software/prism/	
Fluidigm Real-Time PCR Analysis Software v4.5.2	Fluidigm/Standard BioTools	https://www.standardbio.com/products/software	
MultiExperiment Viewer 4.9.0	MeV Development Team	https://webmev.tm4.org/about	

immunosuppressed were instead mock-treated with sterile PBS, the diluent used for the triamcinolone acetonide.

For the downstream EdU labeling assay, we infected two additional groups of fish with 50,000 BSs per fish, and mock-infected one more group. One group was mock-infected with RPMI 1640 (n = 27) and served as a control for the second group infected with *S. molnari* (n = 36). The final third group was divided into six sub-groups (n = 4 each) for the purpose of memory B cell detection.

To measure differential gene expression, 50 fish were infected with one million BSs each, five fish for each of ten sampling timepoints, sampled at one-week intervals for the ten-week duration of the experiment. An additional five non-infected fish were dissected immediately prior to commencing the infection trial, and they served as the control group.

A final independent cohort was infected with 50,000 BSs per fish before immunosuppression rather than immunosuppressed first. We subjected this group to a 223-day gap between infection and treatment with triamcinolone acetonide (as described above) to study immunological memory.

4.4 Measuring peripheral blood B cell concentration

We collected minimal quantities (around 50 to 100 µL) of blood from experimental fish at a frequency of twice weekly throughout the 6-week experiment. The blood was collected with 30-gauge needles into heparinized syringes (via rinsing of the needle and syringe with 200-300 µL of 5,000 IU/mL heparin sodium before use). In preparation for flow cytometry, 4 µL of the whole blood specimens were aliquoted, the blood was resuspended in 200 µL of RPMI 1640 before 100 µL was discarded. Preparation of specimens for flow cytometry was in the 96-well plate format. We centrifuged the cells at 500 *g* for 3 min and washed them once more to dilute and remove any serum (all washes and stains were in the absence of antibiotics or bovine serum). In parallel, 2 µL of the whole blood was collected in TNES-urea to measure parasitemia. The remainder of the heparinized blood was centrifuged at 500 *g* for 5 min. We collected and froze the plasma at -20°C until necessary for downstream applications.

For flow cytometry, the cells were then stained with previously titrated SP2/0 hybridoma supernatant containing the monoclonal anti-carp IgM antibody (clone WCI12) (57) diluted 1:100 in RPMI 1640. We incubated cells for 20 min in ice before subjecting cells to two washes to remove excess antibodies. 1:500 goat anti-mouse IgG1-APC (Abcam, Cambridge, UK) was then applied as a secondary detection reagent, also diluted in RPMI 1640. Incubation was for 20 min in ice before we spun cells down, and added 3,3'-dihexyloxacarbocyanine iodide [DiOC6(3)] (Life Technologies, Carlsbad, CA, USA) diluted to 5 µg/mL in RPMI 1640. We used this lipophilic dye as an alternative to any density centrifugation step, to distinguish the relatively metabolically active and endoplasmic reticulum- or mitochondria-rich leukocytes from the relatively inactive red blood cells. All stains were performed in a volume of 100 µL. A final centrifugation took place before we resuspended cells in a final volume of 200 µL of RPMI 1640. The cells were measured on the BD FACSCanto II (BD Biosciences, Prague, Czech Republic) and data was recorded for 20 s at a medium flow rate (60 µL/min) for all samples, allowing us to quantify both proportion and absolute numbers of B cells in the original 2 µL of whole blood.

We used a two-laser configuration of the BD FACSCanto II: equipped with a 488-nm blue laser and a 633-nm red laser.

4.5 Enzyme-linked immunosorbent assay (ELISA) measurement of relative antibody titre

We designed an indirect ELISA and calculated the relative antibody titre from each fish plasma sample according to a method established by Sacks et al. (58). Our objective was to quantify the amount of *S. molnari*-specific IgM in fish plasma and hence the antigen coating remained constant throughout the experiment. We collected and pooled together parasite lysate derived from three different individual fish at a 1:1:1 mass ratio. Live parasite BSs were pelleted and resuspended in phosphate-buffered saline (PBS) supplemented with the cOmplete Protease Inhibitor Cocktail (Roche Diagnostics GmbH, Mannheim, Germany) by adding one part (volume-wise) of the manufacturer's recommended stock solution to 24 parts of PBS. This suspension was subjected to a

minimum of three freeze-thaw cycles before the lysate was centrifuged at 13,000 *g* for 10 min at 4°C. We collected the supernatant and measured the absorbance at 280 nm to estimate the protein content using a NanoDrop 2000 (Thermo Fisher Scientific, Wilmington, DE, USA). This exact antigen pool was aliquoted and frozen until all plasma samples were collected for the ELISA.

The *S. molnari* antigen was diluted to 25 µg/mL in 29 mM Na_2CO_3 71 mM $NaHCO_3$ pH 9.6 coating buffer. 100 µL were added to wells of a 96-well flat-bottom immunoGrade plates (Carl Roth GmbH, Karlsruhe, Germany) and left to incubate overnight at 4°C. The coating solution was decanted the next day and 100 µL of PBS 5% non-fat dry milk powder (5 g/100 mL) was added to each well. We left the plate blocking at ambient temperature for 3 hours. We washed away the blocking buffer three times using 100 µL of PBS 0.1% Tween-20. We then added either 50 µL of PBS (for background subtraction) or experimental fish plasma diluted in PBS in triplicate. The specific details of fish plasma dilution and which samples to include on each plate are explained by Sacks et al. (58). Briefly, a dilution series of a seropositive fish plasma from another experiment served as a standard and was included on every plate (59). We measured the specific antibody titre of this specimen in an independent experiment through a two-fold plasma dilution series. The last dilution with an absorbance above the mean absorbance plus two SDs of a seronegative SPF naïve cohort (n = 5, plasma diluted 1:100) was considered the antibody titre of the standard. We ensured that we had enough of this plasma for every plate we intended to run onwards. Thus, a two-fold dilution series of the standard, ranging from 1:200 to 1:12,800, was included on every plate for the purpose of determining the relative antibody titre and to account for inter-assay and -plate variation. The experimental fish plasma was generally diluted either 1:100 for the naïve group or 1:200 for the infected group, provided the absorbance at 450 nm (A450nm) fell within the range of the standard curve. Otherwise, a specimen was assayed again at a higher or lower dilution as appropriate. The plasma was incubated for 1 hour at ambient temperature. It was washed away thrice with PBS 0.1% Tween-20. We repeated these incubation steps sequentially with a 100 µL of secondary mouse anti-carp IgM antibody (clone WCI12 supernatant diluted 1:2000 in PBS) and a tertiary anti-mouse IgG-horse radish peroxidase conjugate antibody diluted 1:5000 (Sigma-Aldrich, Darmstadt, Germany) before a final wash step (five washes) and signal development by adding 100 µL of pre-warmed TMB per well (Thermo Fisher Scientific, Rockford, IL, USA). The plates were incubated for 6 min before we stopped the reaction with 2 M sulfuric acid.

We measured the A450nm on the Infinite 200 PRO microplate reader (Tecan, Männedorf, Switzerland). Before analysis, all measurements were background-corrected by subtracting the mean of the triplicate PBS internal negative control measurements included on every plate.

4.6 qPCR quantification of parasitemia

We extracted total DNA from 2 µL of whole blood. The blood was immediately stored in 400 µL of TNES-urea (10 mM Tris-HCl, 125 mM NaCl, 10 mM EDTA, 0.5% SDS, and 4 M urea, pH 8.0) at 4°C. Once the entirety of samples for the experiment had been collected, the DNA was purified via a modified phenol-chloroform extraction as described by Holzer et al. (60). We measured the yield and the purity via spectrophotometry (ratio of absorbance at 260 nm to 280 nm) using the NanoDrop 2000 (Thermo Fisher Scientific, Wilmington, DE, USA). All samples were diluted to 100 ng/µL to normalize the input material for the qPCR. We measured relative parasitemia as the quantity of *S. molnari* SSU rDNA relative to *C. carpio* β-actin DNA using the primers and probes in a duplex TaqMan real-time PCR assay as described previously (26). Naturally, severe disease would both increase parasitemia and deplete host erythrocytes (32), increasing the parasite signal while decreasing the host signal. In all instances and timepoints for the mock-infected group, and for some of the earlier timepoints in infected groups, no parasite was detectable, no PCR product was amplified, and no Ct value was measurable. For these specimens, to enable relative quantification, we assigned them a Ct value of 50, the number of PCR cycles we programmed. Instead of omitting these specimens, we could include them in analyses with Ct values measured from infected specimens. Measurements were made in technical duplicates. The TaqMan qPCR was performed on the QuantStudio 6 (Applied Biosystems, Foster City, CA, USA).

4.7 EdU pulse labeling of proliferating and memory B cells

Experimental fish were injected with the thymidine analogue EdU to measure cells proliferating *in vivo* during the acute response to *S. molnari*. The fish in these two groups were each injected intraperitoneally with 100 µL of 5 mM EdU (diluted in a 1:1 sterile solution of distilled H_2O and RPMI 1640) one day before sampling. We sampled four infected and three mock-infected fish per week at one-week intervals between weeks 1 and 9 post-infection.

A separate group of fish was instead injected three times (at two-day intervals) during a single labeling window/week between weeks 3 and 8 of this experiment. The purpose was to capture the long-term outcome of the proliferation and EdU incorporation events that had occurred during a particular labeling window between different organs and between different windows. Therefore, we sampled these fish approximately six months after each respective labeling window.

The entirety of the head kidney and spleen were biopsied. We placed the tissues upon the surfaces of 100-µm cell strainers (Corning, Durham, NC, USA). The tissues were then gently dissociated using the textured end of a syringe plunger with simultaneous washing and rinsing with RPMI 1640. The cell suspensions were then loaded onto 25% Percoll (Cytiva, Uppsala, Sweden), prepared with one part Percoll and three parts RPMI 1640. The heparinized blood was loaded onto Ficoll-Paque (Cytiva, Uppsala, Sweden). Leukocytes were enriched by density centrifugation at 500 *g* for 20 min at 4°C with minimum acceleration and braking. We collected either the pellet for splenocytes and head kidney leukocytes, or the buffy coat for blood mononuclear cells. These cell fractions were washed twice in RPMI 1640. We enumerated the cells by Trypan Blue exclusion in a Bürker chamber. One million were allotted per fish per compartment, they were stained for detection of IgM^+ cells as described for blood leukocytes in section 4.4 minus the DiOC6(3) staining.

Cells that had incorporated EdU were detected using the Click-iT EdU Alexa Fluor 488 Flow Cytometry Assay Kit (Life Technologies Limited, Paisley, UK) according to the manufacturer's instructions except that the entire protocol was conducted on 96-well non-tissue culture-treated polystyrene V-bottom plates (Greiner Bio-One, Les Ulis, France) with the maximum wash volumes adjusted accordingly: we used 10% of the recommended freshly prepared Click-iT cocktail per specimen, and hence resuspended the cells in only 10 µL of saponin-based permeabilization and wash reagent in the step prior to the Click-iT reaction. Specimens were analyzed on the BD FACSCanto II.

4.8 Primer selection

For SYBR Green-based qPCR, the *igm*-specific primer pairs (against both *membIgM* and *secIgM*) and housekeeping *bactin*-specific primer pairs were previously described (26). We designed the other hypothetical/predicted markers of B cell activation/differentiation and they are described in Supplementary Table S1.

For the multiplex qPCR, the gene/primer selection was based on a single-cell RNA sequencing B cell atlas published for grass carp *Ctenopharyngodon Idella* (16). The nucleotide sequences of the B cell-specific target genes in common carp were derived from the respective NCBI nucleotide accession using the Pyrosequencing assay design software (Biotage AB, Uppsala, Sweden). For each of the 18 target genes, we designed either the sense or the antisense primer to bind an exon-exon junction. They are outlined in Supplementary Table S1. *eef1a1* (eukaryotic translation elongation factor 1 alpha 1) and *rps11* (ribosomal protein S11) were included as reference genes (61).

4.9 Quantitative reverse transcription PCR gene expression profiling of B cell activation and differentiation markers

Fish were dissected and the B cells stained with monoclonal anti-carp IgM antibody (clone WCI12) as described for the proliferation assay. MACS was performed according to the manufacturer's instructions using Anti-Mouse IgG Microbeads (Miltenyi Biotec, Bergisch Gladbach, Germany). Cells were stored in RNAlater (Thermo Fisher Scientific Baltics UAB, Vilnius, Lithuania) overnight, centrifuged the next day at 5,000 *g* either undiluted or diluted 1:1 with PBS. We then stored the pellet at -20°C for RNA isolation using the NucleoSpin RNA kit (MACHEREY-NAGEL, Düren, Germany) according to the manufacturer's instructions. RNA was aliquoted for long-term storage at -80°C or to prepare a 4 ng/µL solution from which 2.5 µL was used (10 ng) in the 10 µL reaction format of the Power SYBR Green RNA-to-CT 1-Step Kit (Thermo Fisher Scientific Baltics UAB, Vilnius, Lithuania) as recommended by the manufacturer. Enough of an equally proportioned pool of 12 randomly selected RNA specimens was prepared and assayed as described above as an inter-run calibrator. We made technical duplicate measurements on the QuantStudio 6 (Applied Biosystems, Foster City, CA, USA). We repeated measurements for any technical duplicates that varied over 0.5 cycles. In this case, Ct values were adjusted based on the inter-run calibrator but otherwise, we followed the sample-maximization method for plate/assay design. We analyzed the data via the $2^{-\Delta\Delta CT}$ method: all data were initially normalized to the Ct values of *bactin* from the same RNA specimen (ΔCt), these data were further normalized to the mean of the ΔCt of the corresponding control group (ΔΔCt).

4.10 Multiplex qPCR gene expression profiling

RNA specimens extracted for one-step RT-qPCR described above were also aliquoted and reverse-transcribed into cDNA using the Reverse Transcription Master Mix (Standard BioTools, San Francisco, CA, USA) in a Thermocycler-T1 (Biometra, Analytik Jena, Jena, Germany) instrument. The resulting cDNA was pre-amplifed using the Preamp Master Mix (Standard BioTools) and a primer master mix with a final concentration of 100 µM per primer pair. Finally, preamplified cDNA was treated with exonuclease I (New England BioLabs, Ipswich, MA, USA) and diluted in SsoFast EvaGreen Supermix with Low ROX (Bio-Rad) and 192.24 DELTAgene Sample Reagent (Standard BioTools).

We used the BioMark HD system (Standard BioTools) to profile the expression of selected B cell marker genes and two reference genes (Supplementary Table S1) in the preamplified cDNA samples. To this end, the primers and pre-amplified cDNAs were inserted to the assay and sample inlets, respectively, on a 192.24 Gene Expression biochip (Standard BioTools). The Control Line Fluid and the Actuation and Pressure Fluid (Standard BioTools) were transferred to the wells provided on the biochip. Having underwent the Load Mix script using the IFC Controller RX (Standard BioTools), the 192.24 Gene-Expression biochip was finally transferred to the BioMark HD-System (Standard BioTools) to perform the quantification reactions.

The Ct values were retrieved using the Fluidigm RealTime PCR Analysis Software v4.5.2 and translated into copy numbers based on external amplicon-specific standard curves ($R^2 > 0.99$). The relative copy numbers were normalised by the geometric mean of the expression values of the suitable reference genes *eef1a1* and *rps11* (61).

4.11 Fixation, permeabilization, and intracellular anti-IgM staining of putative plasma cells

For detection of antibody-secreting cells, we used head kidney biopsies from non-IS fish that received either 50,000 or 250,000 *S. molnari* BSs. Tissue processing and staining for membrane-bound/cell surface IgM was as described above but we started with five million cells in anticipation of detecting rare cell populations.

To costain for cell surface and intracellular IgM, we used the same anti-carp IgM clone WCI12 antibody specially purified from supernatant with the Mouse TCS Antibody Purification kit (Abcam, Cambridge, UK) according to the manufacturer's instructions. The antibody was then biotinylated using EZ-Link Sulfo-NHS-LC-

Biotin (Thermo Fisher Scientific, Rockford, IL, USA) according to the manufacturer's instructions with a 100-fold molar excess of biotin. The prepared antibody (WCI12-biotin) was then dialyzed against a 1000-fold volume excess of PBS. The successful biotinylation reaction was confirmed by flow cytometry and western blot using streptavidin reagents (data not shown).

After cell surface staining, we washed the cells twice with Hanks' Balanced Salt Solution (HBSS) (Thermo Fisher Scientific, Paisley, UK) supplemented with 1% fetal bovine serum. We then fixed the cells in 100 µL of IC Fixation Buffer (Thermo Fisher Scientific, Carlsbad, CA, USA) for 30 min at ambient temperature. From this point onwards, we pelleted cells by centrifugation at 800 *g* for 5 min. The cells were then washed twice with HBSS 1% fetal bovine serum before permeabilization for 15 min at ambient temperature with Permeabilization Buffer (Thermo Fisher Scientific, Carlsbad, CA, USA). After this fixation and permeabilization, we pelleted cells and incubated them for 30 min in Permeabilization Buffer with 5% heat-inactivated BALB/C mouse serum to saturate the existing anti-mouse IgG reagent used for membrane IgM staining. The cells were pelleted and stained in the refrigerator overnight with 300 ng of WCI12-biotin per specimen.

We washed cells twice with Permeabilization Buffer. Cells were then stained with 120 µL of streptavidin PE-Cyanine7 conjugate (Thermo Fisher Scientific, Carlsbad, CA, USA) diluted 1:500 in Permeabilization Buffer for 30 min in ice. The excess streptavidin reagent was washed away twice in Permeabilization Buffer before we resuspended cells for flow cytometry analysis.

4.12 Quantification and statistical analysis

All statistical details of experiments can be found in either the figure legends, or in the supplementary figures and their respective legends.

Throughout this study, statistical significance was always defined by a P value of less than 0.05 or a less than 5% probability of the null hypothesis being true. We used these abbreviations to further specify the outcomes of all statistical tests we performed: ns (not significant); * $p < 0.05$; ** $p < 0.01$; *** $p < 0.001$; **** $p < 0.0001$.

Data availability statement

The original contributions presented in the study are included in the article/Supplementary Material, further inquiries can be directed to the corresponding author/s.

Ethics statement

The animal study was approved by Ministry of Education, Approval ID: MSMT-4186/2018-2. The study was conducted in accordance with the local legislation and institutional requirements.

Author contributions

JC: Conceptualization, Formal analysis, Investigation, Methodology, Visualization, Writing – original draft, Writing – review & editing. AP-S: Conceptualization, Investigation, Methodology, Writing – review & editing. ND: Investigation, Writing – review & editing. JM: Investigation, Writing – review & editing. AR: Investigation, Writing – review & editing, Conceptualization, Data curation, Formal analysis, Methodology, Supervision, Visualization. AH: Conceptualization, Supervision, Writing – review & editing, Funding acquisition, Project administration. TK: Conceptualization, Funding acquisition, Project administration, Supervision, Writing – review & editing, Investigation, Methodology.

Funding

The author(s) declare financial support was received for the research, authorship, and/or publication of this article. We would like to acknowledge: the Ministry of Education, Youth and Sports-Interaction, USA of the Czech Republic (MŠMT- LTAUSA) for funding this work through the project LTAUSA19108 granted to TK; the Czech Science Foundation (GAČR) for funding this work through the projects 19-25589Y and 23-08042K granted to TK, and 19-28399X granted to AH.

Acknowledgments

We would also like to acknowledge Mrs. Joana Pimentel for the care, effort, and attention she dedicated to fish husbandry and to this study.

Conflict of interest

The authors declare that the research was conducted in the absence of any commercial or financial relationships that could be construed as a potential conflict of interest.

Publisher's note

Supplementary material

The Supplementary Material for this article can be found online at: https://www.frontiersin.org/articles/10.3389/fimmu.2024.1493840/full#supplementary-material

References

1. Flajnik MF. A cold-blooded view of adaptive immunity. *Nat Rev Immunol*. (2018) 18:438–53. doi: 10.1038/s41577-018-0003-9

2. Pradeu T, Du Pasquier L. Immunological memory: What's in a name? *Immunol Rev*. (2018) 283:7–20. doi: 10.1111/imr.12652

3. Perey DY, Finstad J, Pollara B, Good RA. Evolution of the immune response. VI. First and second set skin homograft rejections in primitive fishes. *Lab Invest*. (1968) 19:591–7.

4. Linthicum DS, Hildemann WH. Immunologic responses of Pacific hagfish. 3. Serum antibodies to cellular antigens. *J Immunol*. (1970) 105:912–8. doi: 10.4049/jimmunol.105.4.912

5. Sigel MM, Voss EWJ, Rudikoff S. Binding properties of shark immunoglobulins. *Comp Biochem Physiol A Comp Physiol*. (1972) 42:249–59. doi: 10.1016/0300-9629(72)90384-2

6. Eve O, Matz H, Dooley H. Proof of long-term immunological memory in cartilaginous fishes. *Dev Comp Immunol*. (2020) 108:103674. doi: 10.1016/j.dci.2020.103674

7. Dooley H, Flajnik MF. Shark immunity bites back: affinity maturation and memory response in the nurse shark, Ginglymostoma cirratum. *Eur J Immunol*. (2005) 35:936–45. doi: 10.1002/eji.200425760

8. Schaperclaus W. Beitrag zur Kenntnis der Punctata-Formen und -Typen und zur Theorie der Entstehung der infektiosen Bauchwassersucht des Karpfens VII Untersuchungen uber die ansteckende Bauchwassersucht des Karpfens und ihre Bekampfung. *Zentralblatt fuer Bakteriologie Jena Abt II*. (1942) 105:49–72.

9. Śnieszko S. Badania bakteriologiczne i serologiczne nad bakteriami posocznicy karpi. *Mémoires de l'Institut d'Ichtyobiologie et Pisciculture de la Station de Pisciculture Experimentale a Mydlniki de l'Université Jagiellonienne a Cracovie*. (1938).

10. Van Muiswinkel WB. A history of fish immunology and vaccination I. The early days. *Fish Shellfish Immunol*. (2008) 25:397–408. doi: 10.1016/j.fsi.2008.02.019

11. Davidson GA, Lin SH, Secombes CJ, Ellis AE. Detection of specific and 'constitutive' antibody secreting cells in the gills, head kidney and peripheral blood leucocytes of dab (*Limanda limanda*). *Vet Immunol Immunopathol*. (1997) 58:363–74. doi: 10.1016/s0165-2427(97)00017-2

12. Ye J, Kaattari IM, Kaattari SL. The differential dynamics of antibody subpopulation expression during affinity maturation in a teleost. *Fish Shellfish Immunol*. (2011) 30:372–7. doi: 10.1016/j.fsi.2010.11.013

13. Ma C, Ye J, Kaattari SL. Differential compartmentalization of memory B cells versus plasma cells in salmonid fish. *Eur J Immunol*. (2013) 43:360–70. doi: 10.1002/eji.201242570

14. Bromage ES, Kaattari IM, Zwollo P, Kaattari SL. Plasmablast and plasma cell production and distribution in trout immune tissues. *J Immunol*. (2004) 173:7317–23. doi: 10.4049/jimmunol.173.12.7317

15. Wu L, Fu S, Yin X, Guo Z, Wang A, Ye J. Long-lived plasma cells secrete high-affinity antibodies responding to a T-dependent immunization in a teleost fish. *Front Immunol*. (2019) 10:2324. doi: 10.3389/fimmu.2019.02324

16. Pan Y, Wu C, Zhong Y, Zhang Y, Zhang X. An atlas of grass carp igM+ B cells in homeostasis and bacterial infection helps to reveal the unique heterogeneity of B cells in early vertebrates. *J Immunol*. (2023) 211:964–80. doi: 10.4049/jimmunol.2300052

17. Picard-Sanchez A, Estensoro I, Del Pozo R, Piazzon MC, Palenzuela O, Sitja-Bobadilla A. Acquired protective immune response in a fish-myxozoan model encompasses specific antibodies and inflammation resolution. *Fish Shellfish Immunol*. (2019) 90:349–62. doi: 10.1016/j.fsi.2019.04.300

18. Mechlaoui M, Nordstrand E, Strandskog G, Jensen I, Seternes T. Vaccinated Atlantic salmon (*Salmo salar* L.) maintain a specific antibody response throughout the seasonal fluctuations of a full commercial production cycle in sea: a case study. *Aquaculture*. (2025) 595:741536. doi: 10.1016/j.aquaculture.2024.741536

19. Born-Torrijos A, Kosakyan A, Patra S, Pimentel-Santos J, Panicucci B, Chan JTH, et al. Method for isolation of myxozoan proliferative stages from fish at high yield and purity: an essential prerequisite for *in vitro*, *in vivo* and genomics-based research developments. *Cells*. (2022) 11:377. doi: 10.3390/cells11030377

20. Dobai T, Bartosova-Sojkova P. Sphaerospora molnari. *Trends Parasitol*. (2024) 40:352–3. doi: 10.1016/j.pt.2023.12.011

21. Siddall ME, Martin DS, Bridge D, Desser SS, Cone DK. The demise of a phylum of protists: phylogeny of Myxozoa and other parasitic cnidaria. *J Parasitol*. (1995) 81:961–7. doi: 10.2307/3284049

22. Holland JW, Okamura B, Hartikainen H, Secombes CJ. A novel minicollagen gene links cnidarians and myxozoans. *Proc Biol Sci*. (2011) 278:546–53. doi: 10.1098/rspb.2010.1301

23. Foox J, Siddall ME. The road to cnidaria: history of phylogeny of the myxozoa. *J Parasitol*. (2015) 101:269–74. doi: 10.1645/14-671.1

24. Yahalomi D, Atkinson SD, Neuhof M, Chang ES, Philippe H, Cartwright P, et al. A cnidarian parasite of salmon (Myxozoa: Henneguya) lacks a mitochondrial genome. *Proc Natl Acad Sci U S A*. (2020) 117:5358–63. doi: 10.1073/pnas.1909907117

25. Abos B, Estensoro I, Perdiguero P, Faber M, Hu Y, Diaz Rosales P, et al. Dysregulation of B cell activity during proliferative kidney disease in rainbow trout. *Front Immunol*. (2018) 9:1203. doi: 10.3389/fimmu.2018.01203

26. Korytar T, Wiegertjes GF, Zuskova E, Tomanova A, Lisnerova M, Patra S, et al. The kinetics of cellular and humoral immune responses of common carp to presporogonic development of the myxozoan Sphaerospora molnari. *Parasit Vectors*. (2019) 12:208–3. doi: 10.1186/s13071-019-3462-3

27. Taggart-Murphy L, Alama-Bermejo G, Dolan B, Takizawa F, Bartholomew J. Differences in inflammatory responses of rainbow trout infected by two genotypes of the myxozoan parasite Ceratonova shasta. *Dev Comp Immunol*. (2021) 114:103829. doi: 10.1016/j.dci.2020.103829

28. Perez-Cordon G, Estensoro I, Benedito-Palos L, Calduch-Giner JA, Sitja-Bobadilla A, Perez-Sanchez J. Interleukin gene expression is strongly modulated at the local level in a fish-parasite model. *Fish Shellfish Immunol*. (2014) 37:201–8. doi: 10.1016/j.fsi.2014.01.022

29. Abd-Elfattah A, Kumar G, Soliman H, El-Matbouli M. Persistence of *Tetracapsuloides bryosalmonae* (Myxozoa) in chronically infected brown trout Salmo trutta. *Dis Aquat Organ*. (2014) 111:41–9. doi: 10.3354/dao02768

30. Houghton G, Matthews RA. Immunosuppression in juvenile carp, *Cyprinus carpio* L.: the effects of the corticosteroids triamcinolone acetonide and hydrocortisone 21-hemisuccinate (cortisol) on acquired immunity and the humoral antibody response to *Ichthyophthirius multifiliis* Fouquet. *J Fish Dis*. (1990) 13:269–80. doi: 10.1111/j.1365-2761.1990.tb00783.x

31. Houghton G, Matthews RA. Immunosuppression of carp (*Cyprinus carpio* L.) to ichthyophthiriasis using the corticosteroid triamcinolone acetonide. *Vet Immunol Immunopathol*. (1986) 12:413–9. doi: 10.1016/0165-2427(86)90148-0

32. Korytar T, Chan JTH, Vancova M, Holzer AS. Blood feast: Exploring the erythrocyte-feeding behaviour of the myxozoan *Sphaerospora molnari*. *Parasite Immunol*. (2019) 12:208. doi: 10.1111/pim.12683

33. Shibasaki Y, Afanasyev S, Fernandez-Montero A, Ding Y, Watanabe S, Takizawa F, et al. Cold-blooded vertebrates evolved organized germinal center-like structures. *Sci Immunol*. (2023) 8:eadf1627. doi: 10.1126/sciimmunol.adf1627

34. Zwollo P. Dissecting teleost B cell differentiation using transcription factors. *Dev Comp Immunol*. (2011) 35:898–905. doi: 10.1016/j.dci.2011.01.009

35. Zwollo P, Mott K, Barr M. Comparative analyses of B cell populations in trout kidney and mouse bone marrow: establishing "B cell signatures. *Dev Comp Immunol*. (2010) 34:1291–9. doi: 10.1016/j.dci.2010.08.003

36. Zwollo P, Haines A, Rosato P, Gumulak-Smith J. Molecular and cellular analysis of B-cell populations in the rainbow trout using Pax5 and immunoglobulin markers. *Dev Comp Immunol*. (2008) 32:1482–96. doi: 10.1016/j.dci.2008.06.008

37. Barr M, Mott K, Zwollo P. Defining terminally differentiating B cell populations in rainbow trout immune tissues using the transcription factor XbpI. *Fish Shellfish Immunol*. (2011) 31:727–35. doi: 10.1016/j.fsi.2011.06.018

38. Tafalla C, Gonzalez L, Castro R, Granja AG. B cell-activating factor regulates different aspects of B cell functionality and is produced by a subset of splenic B cells in teleost fish. *Front Immunol*. (2017) 8:295. doi: 10.3389/fimmu.2017.00295

39. Granja AG, Holland JW, Pignatelli J, Secombes CJ, Tafalla C. Characterization of BAFF and APRIL subfamily receptors in rainbow trout (*Oncorhynchus mykiss*). Potential role of the BAFF / APRIL axis in the pathogenesis of proliferative kidney disease. *PloS One*. (2017) 12:e0174249. doi: 10.1371/journal.pone.0174249

40. Chakravarti R, Adams JC. Comparative genomics of the syndecans defines an ancestral genomic context associated with matrilins in vertebrates. *BMC Genomics*. (2006) 7:83–3. doi: 10.1186/1471-2164-7-83

41. Zwollo P. Why spawning salmon return to their natal stream: the immunological imprinting hypothesis. *Dev Comp Immunol*. (2012) 38:27–9. doi: 10.1016/j.dci.2012.03.011

42. Igarashi H, Medina KL, Yokota T, Rossi MID, Sakaguchi N, Comp PC, et al. Early lymphoid progenitors in mouse and man are highly sensitive to glucocorticoids. *Int Immunol*. (2005) 17:501–11. doi: 10.1093/intimm/dxh230

43. Akkaya M, Kwak K, Pierce SK. B cell memory: building two walls of protection against pathogens. *Nat Rev Immunol*. (2019). doi: 10.1038/s41577-019-0244-2

44. Kurosaki T, Kometani K, Ise W. Memory B cells. *Nat Rev Immunol*. (2015) 15:149–59. doi: 10.1038/nri3802

45. Inoue T, Kurosaki T. Memory B cells. *Nat Rev Immunol*. (2024) 24:5–17. doi: 10.1038/s41577-023-00897-3

46. Ye J, Kaattari I, Kaattari S. Plasmablasts and plasma cells: reconsidering teleost immune system organization. *Dev Comp Immunol*. (2011) 35:1273–81. doi: 10.1016/j.dci.2011.03.005

47. Yu X, Tsibane T, McGraw PA, House FS, Keefer CJ, Hicar MD, et al. Neutralizing antibodies derived from the B cells of 1918 influenza pandemic survivors. *Nature*. (2008) 455:532–6. doi: 10.1038/nature07231

48. Weisel FJ, Zuccarino-Catania GV, Chikina M, Shlomchik MJ. A temporal switch in the germinal center determines differential output of memory B and plasma cells. *Immunity*. (2016) 44:116–30. doi: 10.1016/j.immuni.2015.12.004

49. Pickering AD, Pottinger TG. Stress responses and disease resistance in salmonid fish: Effects of chronic elevation of plasma cortisol. *Fish Physiol Biochem*. (1989) 7:253–8. doi: 10.1007/BF00004714

50. Ye J, Bromage ES, Kaattari SL. The strength of B cell interaction with antigen determines the degree of IgM polymerization. *J Immunol*. (2010) 184:844–50. doi: 10.4049/jimmunol.0902364

51. Maule AG, Schreck CB. Glucocorticoid receptors in leukocytes and gill of juvenile coho salmon (*Oncorhynchus kisutch*). *Gen Comp Endocrinol*. (1990) 77:448–55. doi: 10.1016/0016-6480(90)90236-F

52. Saha NR, Usami T, Suzuki Y. A double staining flow cytometric assay for the detection of steroid induced apoptotic leucocytes in common carp (Cyprinus carpio). *Dev Comp Immunol*. (2003) 27:351–63. doi: 10.1016/s0145-305x(02)00116-7

53. Vijay R, Guthmiller JJ, Sturtz AJ, Surette FA, Rogers KJ, Sompallae RR, et al. Infection-induced plasmablasts are a nutrient sink that impairs humoral immunity to malaria. *Nat Immunol*. (2020) 21:790–801. doi: 10.1038/s41590-020-0678-5

54. Holzer AS, Piazzon MC, Barrett D, Bartholomew JL, Sitja-Bobadilla A. To react or not to react: the dilemma of fish immune systems facing myxozoan infections. *Front Immunol*. (2021) 12:734238. doi: 10.3389/fimmu.2021.734238

55. Holzer AS, Bartosova-Sojkova P, Born-Torrijos A, Lovy A, Hartigan A, Fiala I. The joint evolution of the Myxozoa and their alternate hosts: A cnidarian recipe for success and vast biodiversity. *Mol Ecol*. (2018) 27:1651–66. doi: 10.1111/mec.14558

56. Roess DA, Zschokke ME, Peacock JS, Barisas BG. Triamcinolone acetonide inhibits lymphocyte differentiation in B cells decorated with artificial antigen receptors. *Biochem Biophys Res Commun*. (1991) 179:1276–80. doi: 10.1016/0006-291x(91)91711-k

57. Secombes CJ, van Groningen JJ, Egberts E. Separation of lymphocyte subpopulations in carp *Cyprinus carpio* L. by monoclonal antibodies: immunohistochemical studies. *Immunology*. (1983) 48:165–75.

58. Sacks JM, Gillette KG, Frank GH. Development and evaluation of an enzyme-linked immunosorbent assay for bovine antibody to *Pasteurella haemolytica*: constructing an enzyme-linked immunosorbent assay titer. *Am J Vet Res*. (1988) 49:38–41.

59. Ganeva VO, Korytar T, Peckova H, McGurk C, Mullins J, Yanes-Roca C, et al. Natural feed additives modulate immunity and mitigate infection with *sphaerospora molnari* (Myxozoa : cnidaria) in common carp: A pilot study. *Pathogens*. (2020) 9:1013. doi: 10.3390/pathogens9121013

60. Holzer AS, Sommerville C, Wootten R. Molecular relationships and phylogeny in a community of myxosporeans and actinosporeans based on their 18S rDNA sequences. *Int J Parasitol*. (2004) 34:1099–111. doi: 10.1016/j.ijpara.2004.06.002

61. Adamek M, Matras M, Rebl A, Stachnik M, Falco A, Bauer J, et al. Don't let it get under your skin! - vaccination protects the skin barrier of common carp from disruption caused by cyprinid herpesvirus 3. *Front Immunol*. (2022) 13:787021. doi: 10.3389/fimmu.2022.787021